GEOLOGICA CARPATHICA, JUNE 2014, 65, 3, 177–194 doi: 10.2478/geoca-2014-0012

Triassic fluid mobilization and epigenetic lead-zinc sulphide mineralization in the Transdanubian Shear Zone (Pannonian Basin, Hungary)

ZSOLT BENKÓ[1]✉, FERENC MOLNÁR[1], MARC LESPINASSE[2], KJELL BILLSTRÖM[3], ZOLTÁN PÉCSKAY[4] and TIBOR NÉMETH[1,5]

[1]Department of Mineralogy, Eötvös Loránd University, Budapest, Hungary; ✉zsoltbenkoo@gmail.com; ferenc.molnar@gtk.fi
[2]University of Lorraine, UMR GeoRessources 7359, CNRS-CREGU BP 239, Bd des Aiguillettes, 54506 Vandoeuvre les Nancy Cedex, France; marc.lespinasse@univ-lorraine.fr
[3]Laboratory of Isotope Geology, Swedish Natural History Museum, Stockholm, Sweden; kjell.billstrom@nrm.se
[4]Institute of Nuclear Research, Hungarian Academy of Sciences, Debrecen, Hungary; zoltan.pecskay@gmail.com
[5]Institute for Geochemical Research, Hungarian Academy of Sciences, Budapest, Hungary; ntibi@geochem.hu

(Manuscript received November 28, 2013; accepted in revised form March 11, 2014)

Abstract: A combined fluid inclusion, fluid inclusion plane, lead isotope and K/Ar radiometric age dating work has been carried out on two lead-zinc mineralizations situated along the Periadriatic-Balaton Lineament in the central part of the Pannonian Basin, in order to reveal their age and genetics as well as temporal-spatial relationships to other lead-zinc-fluorite mineralization in the Alp-Carpathian region. According to fluid inclusion studies, the formation of the quartz-fluorite-galena-sphalerite veins in the Velence Mts is the result of mixing of low (0–12 NaCl equiv. wt. %) and high salinity (10–26 $CaCl_2$ equiv. wt. %) brines. Well-crystallized (R3-type) illite associated with the mineralized hydrothermal veins indicates that the maximum temperature of the hydrothermal fluids could have been around 250 °C. K/Ar radiometric ages of illite, separated from the hydrothermal veins provided ages of 209–232 Ma, supporting the Mid- to Late-Triassic age of the hydrothermal fluid flow. Fluid inclusion plane studies have revealed that hydrothermal circulation was regional in the granite, but more intensive around the mineralized zones. Lead isotope signatures of hydrothermal veins in the Velence Mts ($^{206}Pb/^{204}Pb$ = 18.278–18.363, $^{207}Pb/^{204}Pb$ = 15.622–15.690 and $^{208}Pb/^{204}Pb$ = 38.439–38.587) and in Szabadbattyán ($^{206}Pb/^{204}Pb$ = 18.286–18.348, $^{207}Pb/^{204}Pb$ = 15.667–15.736 and $^{208}Pb/^{204}Pb$ = 38.552–38.781) form a tight cluster indicating similar, upper crustal source of the lead in the two mineralizations. The nature of mineralizing fluids, age of the fluid flow, as well as lead isotopic signatures of ore minerals point towards a genetic link between epigenetic carbonate-hosted stratiform-stratabound Alpine-type lead-zinc-fluorite deposits in the Southern and Eastern Alps and the studied deposits in the Velence Mts and at Szabadbattyán. In spite of the differences in host rocks and the depth of the ore precipitation, it is suggested that the studied deposits along the Periadriatic-Balaton Lineament in the Pannonian Basin and in the Alps belong to the same regional scale fluid flow system, which developed during the advanced stage of the opening of the Neo-Tethys Ocean. The common origin and ore formation process is more evident considering results of large-scale palinspastic reconstructions. These suggest, that the studied deposits in the central part of the Pannonian Basin were located in a zone between the Eastern and Southern Alps until the Early Paleogene and were emplaced to their current location due to northeastward escape of large crustal blocks from the Alpine collision zone.

Key words: Triassic, Velence Mts, Szabadbattyán, Periadriatic-Balaton Lineament System, lead isotopes, fluid inclusions, Alpine-type epigenetic lead-zinc mineralization.

Introduction

The Periadriatic-Balaton Lineament (PABL) is a major dextral shear zone in the Alpine-Carpathian orogeny that is dividing the Eastern and the Southern Alps in the west, as well as the ALCAPA (Alp-Carpathian-Pannonian) and Zagorje-Mid-Transdanubian Units along its eastern section (Fig. 1). The structurally deformed zone of the PABL was a principal channel of magma and fluid flow in various geotectonic situations, from the Mesozoic onwards. The formation of Cretaceous lamprophyric magmatism (Eisenkappel, Velence Mts), Paleogene and Neogene intermediate magmatism (Recsk, Velence Mts), diorite intrusions and stratovolcanoes (Zala Basin volcanics in the Pannonian Basin; Adamello, Berger plutons; Pohorje intrusions in the Alps; Fig. 1) as well as various types of mineralization (Cu-porphyry, epithermal, lead-zinc epigenetic at Recsk and in the Velence Mts) is clearly or apparently controlled by the repeated reactivation of this fault system.

Along the eastern segment of the PABL, in the central part of the Pannonian Basin two Paleozoic, allochthonous complexes, the Szabadbattyán Block and the Velence Mts crop out. The western part of the Velence Mts is built up of early Permian monzogranite, which is the host of vein-type fluorite-galena-sphalerite-calcite mineralization (hereinafter base-metal-fluorite veins). The near-by (30 km) Szabadbattyán Block is composed of structurally deformed Paleozoic metasedimentary rocks and Triassic andesitic intrusions. The Devonian limestone at Szabadbattyán is host of vein-, and metasomatic-type Pb mineralization.

The age and origin of both mineralizations have been controversial for a long time (Velence Mts: Jantsky 1957; Kaszanitzky 1958; Horvát Ódor 1984; Molnár 1996, 2004,

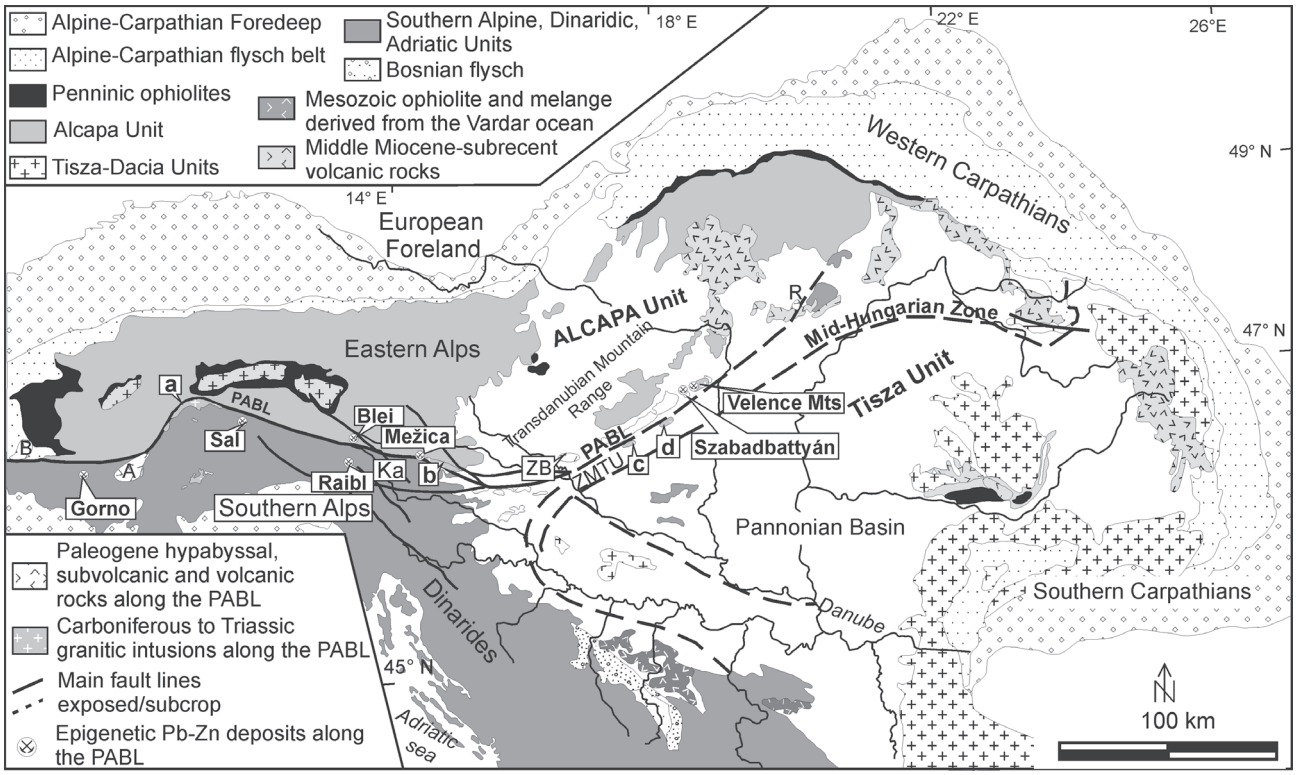

Fig. 1. Geological overview map of the Alp-Carpathian region compiled after Kovács et al. (2007) and Köppel (1983). **Abbreviations:** Faults: **PABL** — Periadriatic Balaton Lineament System. Epigenetic lead-zinc deposits along the PABL: **Sal** — Salafossa, **Blei** — Bleiberg. Paleogene plutons and volcanites: **A** — Adamello Pluton, **B** — Bergell Pluton, **ZB** — Zala Basin, **R** — Recsk. Carboniferous to Permian granite intrusions along the PAL: **a** — Bressanone Pluton, **b** — Eisenkappel Pluton, **c** — Buzsák, **d** — Ságvár, **Ka** — Karawanken Mts. Tectonic units: **ZMTU** — Zagorje–Mid Transdanubian Unit.

Table 1: Summary of magmatic and hydrothermal processes and their characteristics in the Velence Mts and Szabadbattyán Block.

	No.	Magmatic or hydrothermal formation	Formation conditions	Method (formation conditions)	Age	Method (age dating)	References
Velence Mts	VIII.	Quartz-barite veins, illitic alteration	>240 °C 30–40 bar	Fluid inclusion studies Clay mineral thermometry	Ol_1 31 Ma	K/Ar age dating on illite	Benkó et al. 2012
	VII.	Cu-porphyry, skarn and epithermal mineralization of the diorite and andesite	>220 °C 100–280 bar	Fluid inclusion studies	Ol_1 29–32 Ma	K/Ar age dating on illite	Molnár 1996, 2004; Molnár et al. 2010; Bajnóczi et al. 2002
	VI.	Diorite intrusion and andesite volcanism			Ol_1 29–32 Ma	K/Ar age dating on amphibole, plagioclase, whole rock	Darida-Tichy 1987; von Blanckenburg 1995; Benedek et al. 2004
	V.	Lamprophyre (monchiquite-spessartite) dykes			K_3 77 Ma	K/Ar age dating on biotite	Horváth & Ódor 1984
	IV.	Quartz-sphalerite-galena-fluorite veins and illite-kaolinite-smectite alteration (Base-metal-fluorite veins)	90–220 °C 1–1.3 kbar	Fluid inclusion studies Clay mineral thermometry	P; T; K (?)	uncertain, only assumptions	Molnár 1996, 2004; Nemecz 1973; Benkó 2008
	III.	Quartz-molybdenite-pyrite-grey ore mineralization	400–500 °C 1.3–2.5 kbar	Fluid inclusion studies	P	interpreted from FI data	Molnár 1997
	II.	Crystallization of pegmatite	500–550 °C 300–400 °C 1.5–2.5 kbar	Two-feldspar thermometry Fluid inclusion studies	P_1	interpreted	Jantsky 1957; Buda 1993; Molnár et al. 1995
	I.	Crystallization of the granite	740–500 °C 2 kbar	Two-feldspar thermometry	P_1 (274 Ma)	K/Ar age dating on biotite U/Pb dating on zircon	Buda 1985, 1993; Buda et al. 2004
Szabadbattyán	III.	Pb-metasomatic mineralization			P; T; E (?)	no age dating	Földvári 1952; Jantsky 1960; Kiss 2003
	II.	Skarn mineralization			T_3 220 Ma	interpreted	Dunkl et al. 2003; Kiss 2003
	I.	Andesite dykes			T_3 220 Ma	K/Ar age dating on amf., fission track of zircon and apatite	Dunkl et al. 2003; Kiss 2003

Szabadbattyán: Kiss 1951; Földvári 1952; Kiss 2003), due to their allochthonous, exotic positions along the PABL.

In order to shed further light on the timing, nature of ore-forming processes and paleogeographical relations of the mineralizations in the two Paleozoic units we have adopted a multi-method approach. Fluid inclusion microthermometry as well as a new method, called Fluid Inclusion Plane (FIP) technique have been performed to extend the existing knowledge about the nature of ore-forming fluids and enable a discussion on the depth of ore formation. Lead isotope data were collected in order to elucidate the timing and the origin of the Pb components in the ore. Furthermore, we have carried out K/Ar radiometric age determinations on hydrothermal clay mineral assemblages and a rock forming mineral surrounding the veins for a better determination of age constraints of ore formation.

Regional geology and hydrothermal processes

The Velence Mts are located along the southern part of the Alcapa Megaunit and the northern side of the PABL (Fig. 1). The Alcapa Megaunit is composed of the metamorphosed Proterozoic to Mesozoic blocks of the Eastern Alps, the Paleozoic low-grade metamorphic and Mesozoic carbonaceous sequences of the Transdanubian Mountain Range (TMR), the Bükk Mts, as well as the crystalline blocks of the Inner Western Carpathians (Fig. 1). By the Oligocene–Early Miocene, the Alcapa Megaunit escaped northeastward from the Alpine collision zone (Kázmér & Kovács 1985; Csontos et al. 1992; Fodor et al. 1998; Haas et al. 2000). The total 350–400 km present day offset can be attributed to the Paleogene to Mid-Late Miocene extension, lateral extrusion and counter-clockwise rotation of the Alcapa Megaunit (Tari 1996; Csontos &

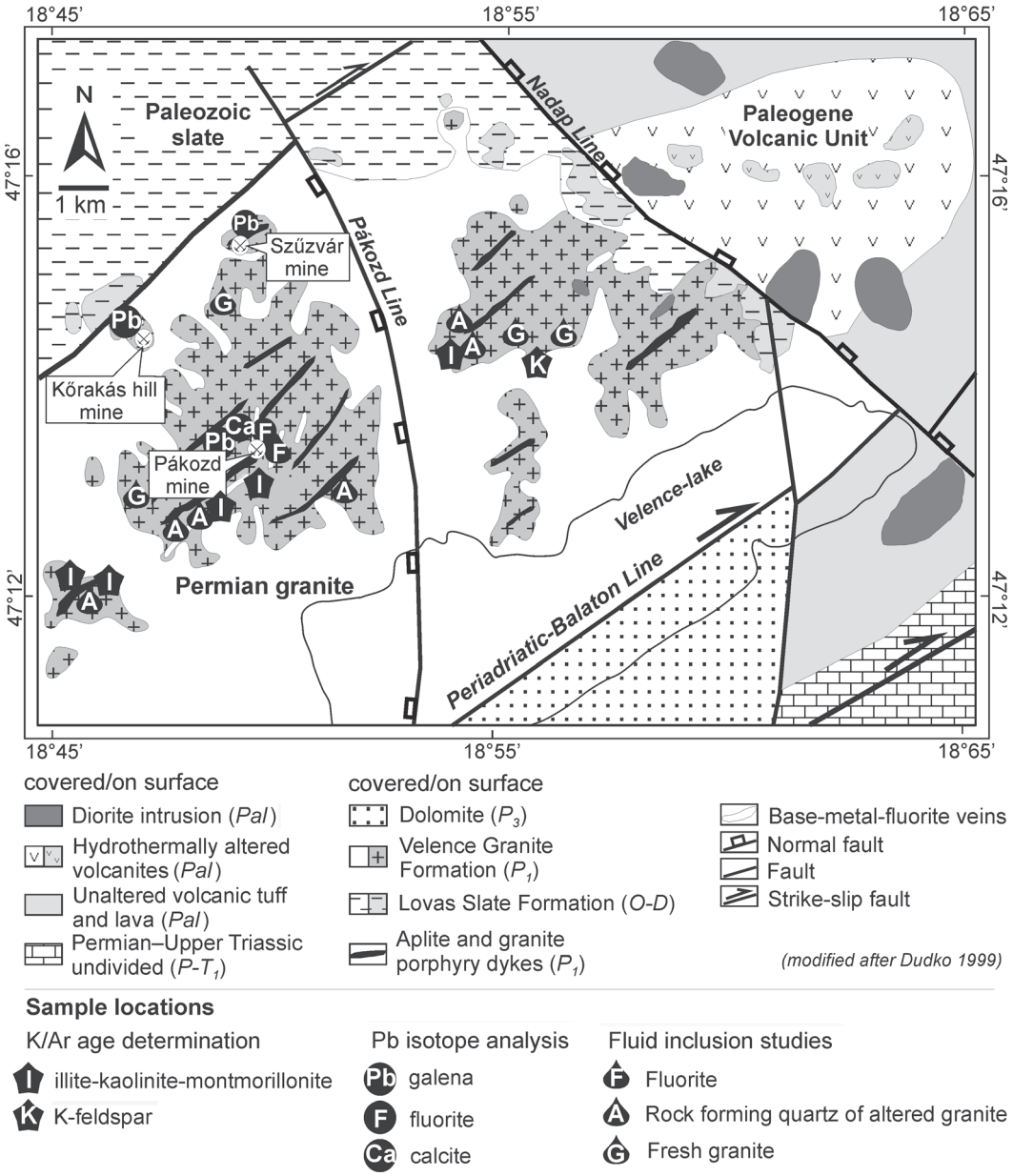

Fig. 2. Geology of the Velence Mts, modified after Dudko (1999) with sample localities of the current study.

Vörös 2004). Along the PABL, Paleozoic and Paleogene units can be regarded as allochthonous blocks in a tectonic mega-mélange between the Alcapa and Zagorje-Mid-Transdanubian Unit (Fig. 1).

The Velence Mts consist of two major units: the western unit is a Permian monzogranite intrusion; the eastern unit is an Early Oligocene intrusive-volcanic complex of intermediate composition (Fig. 2). The granite intrusion can be further divided into two blocks. The boundary between the eastern and the western part of the granite intrusion is the Pákozd Line which is a post-Triassic normal fault (Benkó 2008). The complete sequence of magmatic and hydrothermal events and *p-T* conditions of the different processes are summarized in Table 1.

The Permian granite is an A-type, peraluminous biotitic monzogranite (Uher & Broska 1994, 1996; Broska & Uher 2000; Finger et al. 2003), which intruded into an early Paleozoic anchimetamorphic slate at 274–290 Ma (Balogh et al. 1983; Buda 1985; Buda et al. 2004). The results of mineralogical and fluid inclusion studies by Molnár (1997) suggested that the superimposing quartz-molybdenite-pyrite-grey ore stockwork mineralization along the contact of the granite and the shale was linked to the post-magmatic hydrothermal system of the granite.

The N–S and NE–SW striking base-metal-fluorite veins occur in the western part of the granite body of the Velence Mts (Fig. 2). These veins are surrounded by argillic alteration (illite, kaolinite, smectite) envelopes (Nemecz 1973; Benkó 2008). Galena and sphalerite are co-genetic phases, whereas fluorite is partially co-genetic, and partly younger than other ore minerals. Characteristic ore textures are cocade and brecciated (Jantsky 1957). According to sulphur isotope studies (Benkó 2008) the maximum temperature of ore formation was around 230–250 °C.

By the time of the Late Cretaceous, the granite was intruded by monchiquite-spessartite dykes (Horváth & Ódor 1984). These dykes were K/Ar dated at 77.6 ± 30 Ma (Balogh et al. 1983). The dykes are not altered and they did not generate hydrothermal alteration in the granite host.

In the eastern part of the Velence Mts, a hydrothermally altered and eroded andesitic stratovolcanic structure (dated by the K/Ar method at 28–30 Ma; Bajnóczi 2003) crops out and this unit is underlain by diorite intrusions (Fig. 2). The Paleogene calc-alkaline igneous rocks are characterized by medium- to high-K content and they are regarded as results of syn- to post-syncollisional magmatism, which occurred by the collision of the Apulian Microplate (of African origin) and the European Plate (Darida-Tichy 1987; von Blanckenburg 1995; Benedek 2002; Benedek et al. 2004).

In the Paleogene Volcanic Unit of the Velence Mts, Cu-porphyry and minor skarn mineralization is spatially linked to the diorite intrusion whereas alteration zones typical for high-sulphidation type epithermal systems are known in the outcrops of the stratovolcano (Molnár 1996, 2004; Bajnóczi et al. 2002; Bajnóczi 2003).

The hydrothermal system of the Paleogene age has also interacted with the Permian granite intrusion in the eastern part of the Velence Mts, east of the Pákozd Line (Molnár 2004; Benkó & Molnár 2004; Benkó et al. 2012). Secondary fluid inclusions that are attributed to the Paleogene fluid circulation in the old granite can easily be recognized in rock forming quartz, because the Paleogene fluid circulation took place under low pressure (max. 150–200 bar) boiling conditions resulting in common occurrences of vapour phase-rich and liquid phase-rich (sometimes halite bearing) fluid inclusions.

The Szabadbattyán Block is a thrusted unit composed of metamorphosed slate, phyllite, and carbonate nappes (Fig. 3). Igneous activity is marked by the presence of Carboniferous granite porphyry dykes, whereas andesite dykes of Triassic age (K/Ar data from Balogh et al. 1983 and Bagdaszarjan 1989) intrude the Polgárdi Limestone Formation (Table 1). The epigenetic base-metal mineralization occurs in fractures and as roughly bedding-parallel metasomatic-replacement bodies in the Polgárdi Limestone Formation. The major ore mineral is galena. Bournonite, sphalerite, chalcopyrite, tetrahedrite and native silver are the most common minerals associated with galena (Szakáll & Molnár 2003).

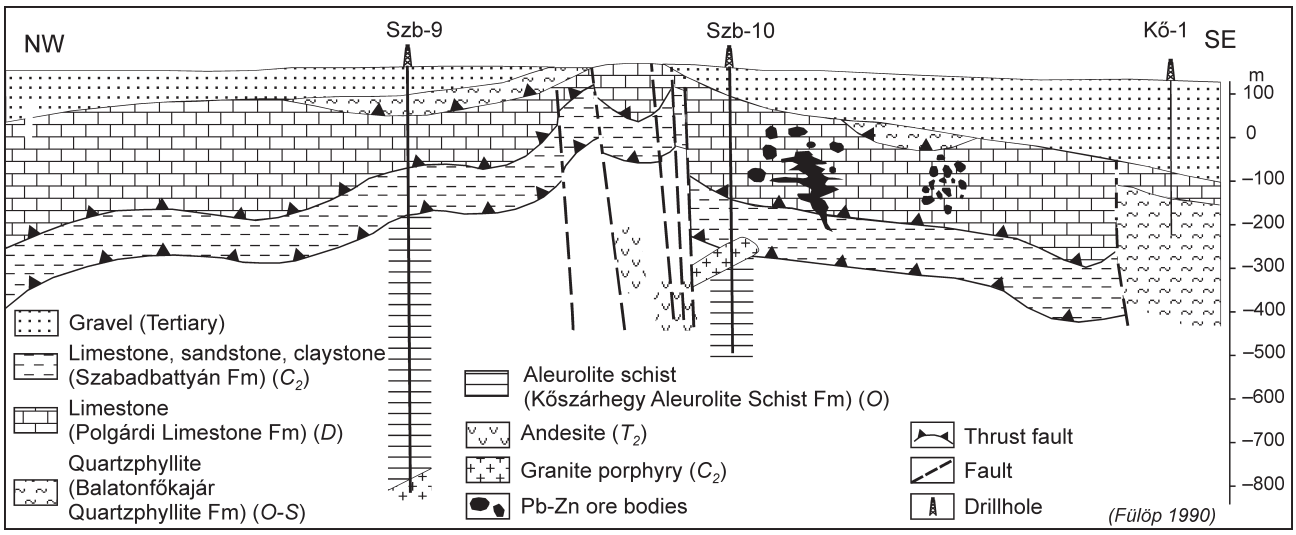

Fig. 3. Section of the Szabadbattyán area (Fülöp 1990).

Sampling and analytical methods

There are no outcrops of the discussed mineralizations therefore no detailed field work has been carried out on these formations. Mineralized samples were collected from the historical Mineralogical Collection of the Eötvös Loránd University, Budapest. Sample localities of rock samples are summarized in Fig. 2.

Fluid inclusion studies have been carried out on quartz, fluorite and sphalerite from the base-metal-fluorite veins in the Velence Mts. For comparison, we also analysed secondary fluid inclusions in rock forming quartz from unaltered granite and from the alteration halo of the hydrothermal veins. To establish the relationships between argillic alteration zones and fluid inclusion assemblages responsible for their formation, the FIP method was applied. In order to determine the extension of the hydrothermal fluid flow, and the rock volume affected by the hydrothermal system, fluid inclusion thermometry and FIP studies have been carried out on the inclusions of the rock forming quartz crystals. Details of the FIP method have been published in Lespinasse & Pecher (1986), Lespinasse & Cathelineau (1990), Lespinasse et al. (2005). Briefly, FIP are Type III extensional microfractures that form always perpendicular on the minimum stress axes of the stress field in rock forming quartz crystals of granitic rocks. If the age of the fluid circulation and hence the age of the FIPs is known one can determine the minimum stress axes of the stress field during fluid flow and mineralization. Another advantage of the method is that FIP density (number of FIP per unit surface, expressed in $1/mm^{-2}$ and cumulative length per unit surface expressed in mm/mm^2) in the rock forming quartz crystals displays a systematic increasing trend towards the alteration zones (e.g. argillic alteration zones, vein swarms; Benkó et al. 2008). Using this approach, secondary fluid inclusions in magmatic quartz crystals of granite can be directly related to certain alteration zones (e.g. argillic alteration) that do not contain hydrothermal minerals with primary fluid inclusions. Fluid inclusion assemblages and FIP density were analysed by the computer code AnIma (Lespinasse et al. 2005), developed at the University of Lorraine, Nancy, France.

Fluid inclusion microthermometric studies were carried out on a Chaixmeca heating–freezing stage. The studies have yielded reproducible temperatures within ±0.1 °C (below 0 °C) and ±1 °C (above 0 °C), respectively. The equipment was standardized with synthetic fluid inclusions (H_2O–CO_2 and pure water) of known microthermometric properties (i.e. triple point temperature for pure CO_2 at –56.6 °C, melting temperature of ice at 0 °C). Thin sections used for fluid inclusion petrography and microthermometry were double polished 100–150 μm thick. Characteristic isochors were calculated using the equations of Zhang & Frantz (1987). The salinities of the aqueous fluid inclusions were calculated using the experimental equation of states of Oakes et al. (1990) and Bodnar (1993).

K/Ar radiometric age determinations were carried out at the Institute of Nuclear Research of the Hungarian Academy of Sciences. Details of the analytical methods can be found in Balogh (1985). Clay mineral phases were collected from alteration selvages of base-metal-fluorite veins cutting the granite and from NE–SW trending clay mineral filled veins. Purity and composition of the mineral fractions were controlled by X-ray powder diffraction (XRPD). After careful separation and mild crushing, the samples were suspended in water glass columns for 200 minutes. Following Stoke's law we then extracted the portion of the suspension which contained the <2 μm size clay mineral fraction. This fraction has the greatest surface area/volume ratio and hence is the most susceptible to diffusion of radiogenic Ar. Nevertheless, several authors presented meaningful K/Ar age data also from <0.2 μm and <0.1 μm size fractions (e.g. Zhao et al. 1997; Zwingmann et al. 2010), especially from sedimentary-diagenetic environments and from shallow fault gauges.

The mineral composition of the clay fraction was determined on the separated, randomly oriented powder samples by semi-quantitative phase analysis. Three aliquots of each sample were separated for diagnostic treatments. Clay minerals were identified by XRD diagrams obtained from parallel-oriented specimens. Diagnostic treatments were carried out for the identification and characterization of the clay minerals. Samples were treated by ethylene-glycol at 60 °C overnight for the detection of swelling clay minerals and mixed layer clay minerals. Magnesium saturation followed by glycerol solvation at 95 °C overnight was used to distinguish smectite and vermiculite. Layer charge of swelling clay minerals was estimated by potassium saturation. Chlorite-kaolinite distinction is based on heating of the samples at 350 and 550 °C for 2 hours. The tetrahedral or octahedral origin of layer charge was determined by the Greene-Kelly test (Greene-Kelly 1953). XRPD measurements were carried out using a Philips PW 1710 diffractometer with CuKα radiation at 45 kV and 35 mA in the lab of the Institute for Geological and Geochemical Research of the Hungarian Academy of Sciences.

Lead isotope measurements were performed on pure galena, calcite and fluorite crystals collected from the base-metal-fluorite veins. Minerals were separated by hand picking under stereomicroscope. The analytical part followed routines adapted at the Swedish Museum of Natural History, Stockholm (DeIgnacio et al. 2006). After dissolution in acids and subsequent ion exchange routines, clean lead separates were yielded. The isotopic analyses were carried out using a Micromass Isoprobe ICP-mass spectrometer in the Swedish Museum of Natural History, Stockholm. Mass bias corrections were accounted for by using an internal Tl normalization, and NBS 981 were run repeatedly to secure data accuracy. Typically, the precision (2σ error) of Pb runs is ±0.10 % or better.

Results

Fluid inclusion petrography and microthermometry

Relatively large (10–20 μm) two phase, liquid–vapour fluid inclusions ratios were detected along the growth zones and in isolated clouds in hydrothermal quartz, in fluorite and in sphalerite crystals in the base-metal-fluorite veins (Fig. 4a,b). The phase ratio between vapour and liquid phases is around 0.1 in the samples from west of the Pákozd Line and around

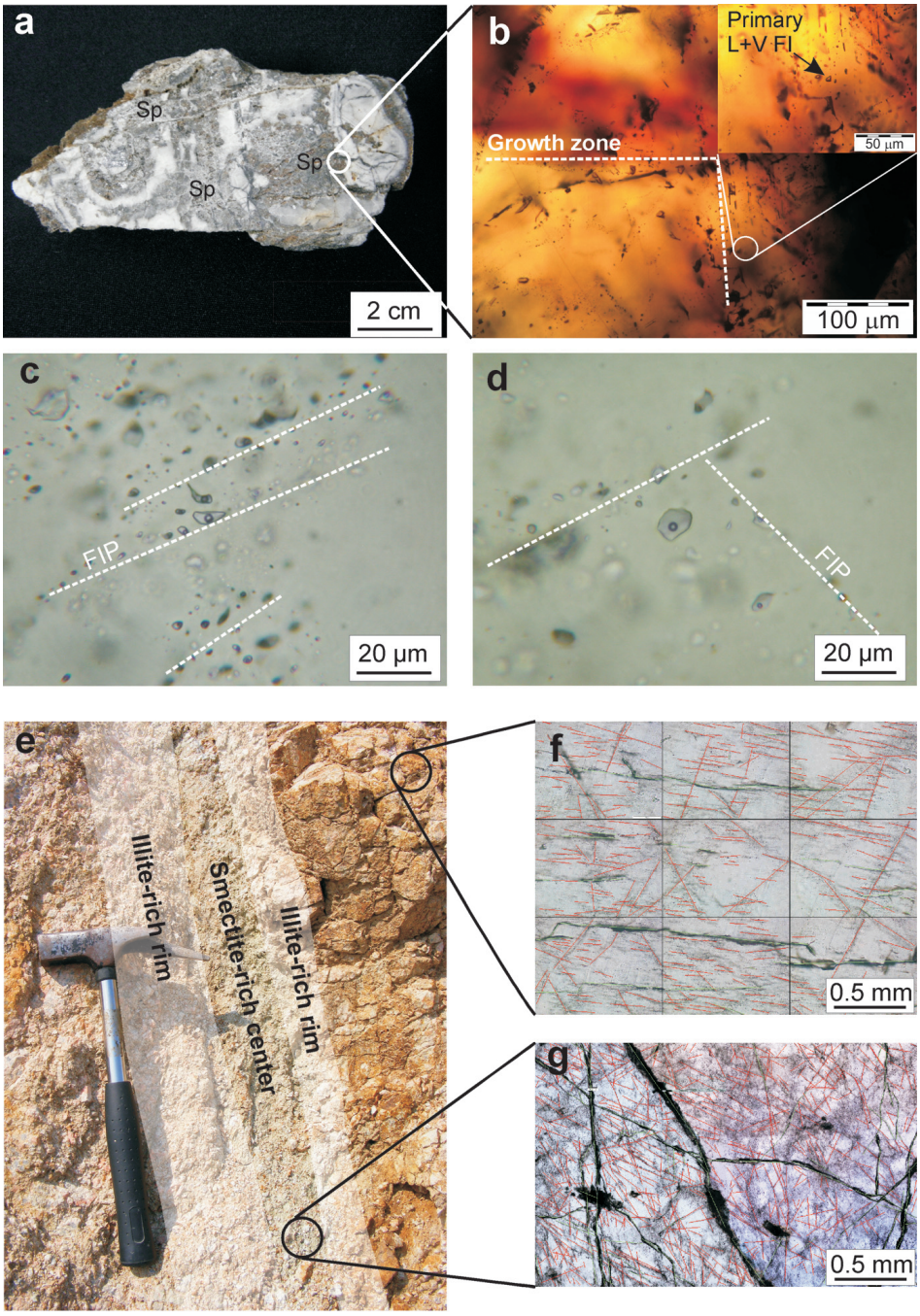

Fig. 4. **a** — Base-metal-fluorite vein with cocade texture from the Velence Mts. The brecciated and altered (illite-kaolinite-smectite) granite is cemented by quartz (white with concentric zonation) and sphalerite (brown). The white circle indicates the place of fluid inclusion studies; **b** — Primary two phase (L+V; liquid-vapor) fluid inclusions along growth zones in sphalerite; **c** — Secondary, two-phase (liquid-vapour) fluid inclusions in rock forming quartz crystals of the granite. The vapour/liquid ratio is 0.2. Fluid inclusions are aligned along fluid inclusion planes; **d** — Secondary, two-phase (liquid-vapour) fluid inclusions in rock forming quartz crystals of the granite. The vapour/liquid ratio is 0.1; **e** — NE-SW trending argillic alteration zone in the western block of the granite. The central part of the alteration zone is greenish due to the smectite whereas the rim is rather white because of the higher relative amount of illite; **f** — FIP in rock forming quartz in unaltered granite. FIP are short and the number of FIP in a certain area is low; **g** — FIP in quartz crystals in altered granite. FIP are long and the number of FIP is high.

0.2 in the samples from east of the Pákozd Line in the hydrothermal quartz. Fluid inclusion data are listed in the Appendix *(as a Supplement in the electronical version; www.geologicacarpathica.com)*.

Two phase liquid-vapour primary fluid inclusions in fluorite from the base-metal-fluorite veins homogenized into liquid phase at temperatures of 90–130 °C in the western block of the granite (e.g. west of the Pákozd Line, Fig. 5a). Considering the eutectic melting temperatures of ice at around –21 °C, their compositions can be modelled in the NaCl–H_2O system. Melting temperatures of ice are distributed between –5.1 °C and –9.8 °C corresponding to 8–13 NaCl equiv. wt. % salinities.

Two phase liquid–vapour primary fluid inclusions in sphalerite homogenized at 80–160 °C in the western unit of the granite (Fig. 5d). Due to their very low eutectic and ice melting temperatures, partly below –60 °C and below –21 °C, respectively, their compositions cannot be modelled in the NaCl–H_2O system. Because of difficulties with the reproducible observations of hydrohalite melting, the fluid composition has been modelled in the $CaCl_2$–H_2O system. Melting of ice took place from –14.8 to –24.5 °C, and the calculated salinities are between 18 and 23 $CaCl_2$ equiv. wt. %.

Primary, two-phase fluid inclusions in the hydrothermal quartz homogenize at 80–130 °C west of the Pákozd Line and 170–220 °C east of the Pákozd line (Fig. 5d). Eutectic

melting in these inclusions started below –50 °C. Therefore salinities of these inclusions were calculated in $CaCl_2$ equiv. wt. %. Final melting temperatures in the inclusions west and east of the Pákozd Line varied from –6.2 °C to –26.4 °C and from –4.3 °C to –21.7 °C, respectively. These final melting temperatures correspond to salinities from 10–25 $CaCl_2$ wt. % and 7–21 $CaCl_2$ wt. %.

Secondary fluid inclusions with similar phase ratios also occur in the rock forming quartz of the granite. Independently of the distance from the alteration zones, these inclusions are regionally present in the granite. However, density of FIP is high in the close vicinity of the veins (53.2–125.1 1/mm^2 and 11.3–26.0 mm/mm^2; Fig. 4e,f) and decreases to the less altered granite (23.9–51.9 1/mm^2 and 4.5–6.9 mm/mm^2;

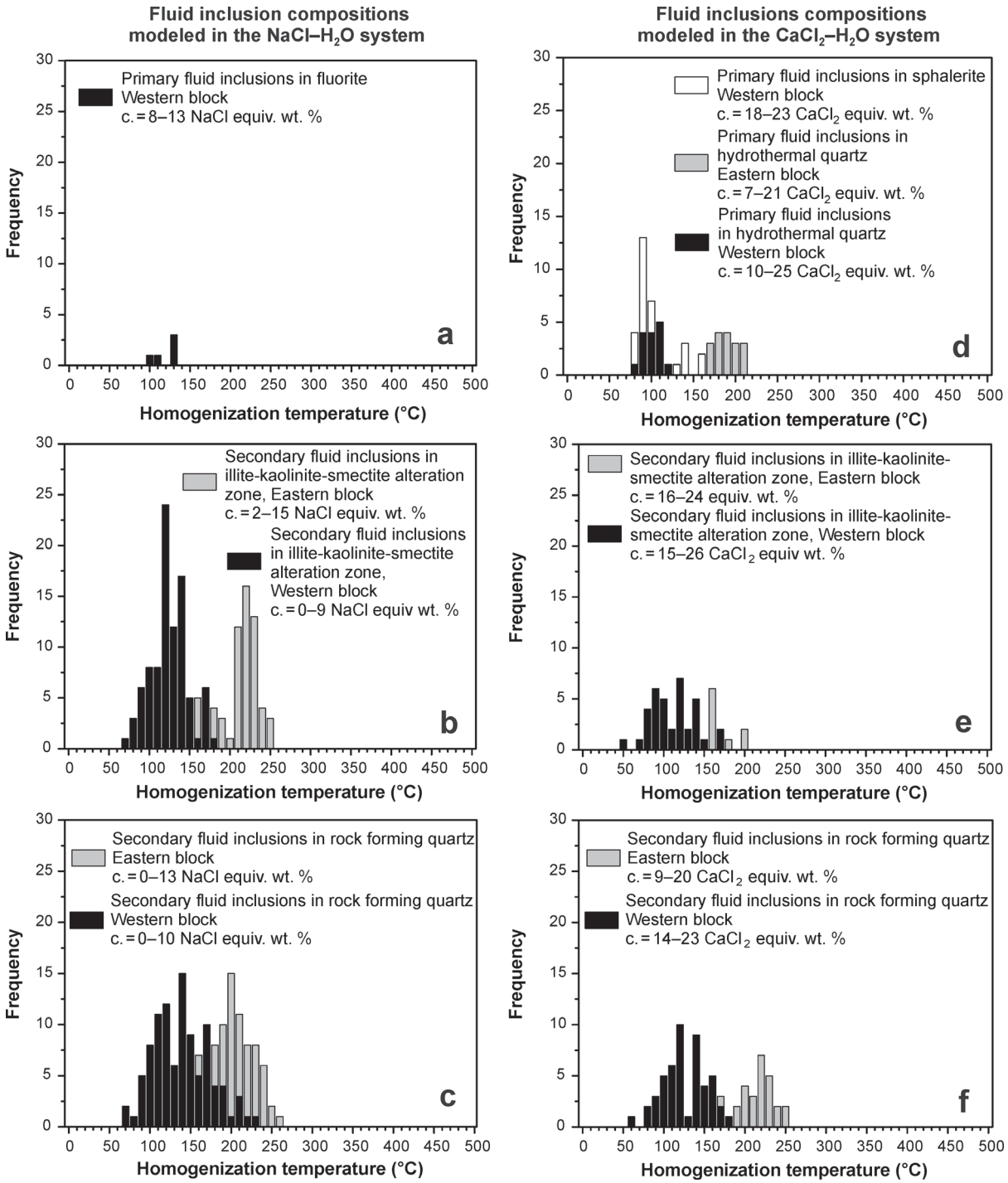

Fig. 5. Homogenization temperature distribution diagram of the measured fluid inclusions in fluorite, sphalerite, hydrothermal quartz, as well as in the rock forming quartz crystals of the granite from the Velence Mts. **a–b–c** — fluid composition is modelled in the NaCl–H_2O system; **d–e–f** — fluid composition is modelled by $CaCl_2$–H_2O system. **c.** — concentration.

Table 2; Fig. 4, e.g). The orientation of the fluid inclusion planes is always parallel to the strike of the base-metal-fluorite veins (NE–SW; Benkó 2008).

One group of secondary fluid inclusions in rock-forming quartz of fresh and argillic altered granite is characterized by eutectic melting temperatures at around –21 °C. The salinities calculated from the melting temperatures of the ice (–0.2 to –8.6 °C) are in the range of 0.3–12 NaCl equiv. wt. %. Homogenization of these inclusions took place into liquid phase at 70–230 °C and 170–260 °C in the western and eastern blocks of the granite, respectively. The median of the homogenization temperatures is around 130 °C in inclusions west of the Pákozd Line and around 210 °C east of the Pákozd Line (Fig. 5b,c).

Table 2: Fluid inclusion plane density data, measured in the rock forming quartz crystals of the Velence Mts granite.

	Locality	FIP density	
		Number of FIP/unit area	Summa lenght of FIP/unit area
Center of illite-kaolinite-smectite alteration zones	1	77.2	11.8
	2	125.1	26
	3	73.9	13.7
	4	53.2	11.3
Out of alteration zones	5	38.9	6.13
	6	23.9	4.5
	7	31.2	6.9
	8	51.9	6.26

Another group of secondary fluid inclusions in rock–forming quartz of fresh and argillic altered granite displayed eutectic melting temperatures from –49 to –56 °C with melting temperatures of the ice between –32.3 °C and –13.6 °C. These fluid inclusions were also modelled in the $CaCl_2$–H_2O system thus calculated salinities are between 9.9 and 25.8 $CaCl_2$ equiv. wt. %. Homogenization temperatures are 50–180 °C and 160 °C –260 °C east and west of the Pákozd Line, respectively. The median of the homogenization temperatures varies similarly to the low salinity secondary fluid inclusions. In the western and eastern block the median is around 135 °C and around 220 °C, respectively (Fig. 5e,f).

Lead isotope data

Lead isotope analyses have been carried out on galena (*n = 4*), fluorite (*n = 4*) and calcite (*n = 2*) from the base-metal-fluorite veins of the Velence Mts and from vein filling galena (*n = 4*) from the Polgárdi Limestone Formation of the Szabadbattyán Block (Figs. 2 and 3). In the Velence Mts, the

Table 3: Lead isotope data of the lead-zinc mineralization in the Velence Mts and at Szabadbattyán. **S–K** — Stacey & Kramers (1975) model age; **C–R** — Cummings & Richards (1975) model age.

Sample number	Analysed mineral	Area	$^{206}Pb/^{204}Pb$	$^{207}Pb/^{204}Pb$	$^{208}Pb/^{204}Pb$	μ value	S-K model age (Ma)	C-R model age (Ma)
BE50301	galena	Velence Mountains	18.288	15.679	38.587	10.06	412	310
BE50806	galena	Velence Mountains	18.278	15.653	38.506	9.95	369	310
BE303030	galena	Velence Mountains	18.305	15.622	38.439	9.80	286	300
BE51339	galena	Velence Mountains	18.268	15.645	38.481	9.91	360	330
BE51041	galena	Velence Mountains	18.363	15.690	38.599			
BE51659	galena	Velence Mountains	18.318	15.660	38.466			
BE50691	galena	Velence Mountains	18.313	15.654	38.443			
BE 51045	fluorite	Velence Mountains	18.438	15.657	38.703			
BE 50691	fluorite	Velence Mountains	18.511	15.697	38.547			
BE 50301	fluorite	Velence Mountains	18.325	15.660	38.499			
BE 51041	fluorite	Velence Mountains	18.457	15.665	38.770			
M06	calcite	Velence Mountains	18.366	16.658	38.545			
M30	calcite	Velence Mountains	18.351	15.663	38.494			
BE50269	galena	Szabadbattyán	18.286	15.667	38.552	10.01	390	310
BE51654	galena	Szabadbattyán	18.339	15.710	38.694	10.19	435	290
BE51664	galena	Szabadbattyán	18.348	15.736	38.781	10.30	477	280
BE50300	galena	Szabadbattyán	18.293	15.679	38.588	10.06	408	310
accuracy: ± 0.10 %								

Table 4: K-Ar radiometric ages of hydrothermal and rock forming minerals from the Velence Mts and Szabadbattyán.

Locality	Rock type and type of hydrothermal alteration	Selected mineral fraction	K-content (%)	^{40}Ar rad/g(cm^3/g)	^{40}Ar rad (%)	K/Ar age (million year)
Pákozd, Big quarry	granite, argillic alteration	illite, kaolinite, smectite	5.010	4.5827×10^{-5}	90.20	**221.2±6.7**
Pákozd, "Pegmatite quarry"	granite, argillic alteration	illite, kaolinite, smectite	4.214	3.6442×10^{-5}	89.30	**209.8±3.7**
Székesfehérvár, Kisfalud quarry, next to the aplite vein	granite, argillic alteration	illite, kaolinite, smectite	3.185	2.8262×10^{-5}	75.00	**214.6±6.7**
Székesfehérvár, Kisfalud quarry	granite, argillic alteration	illite, kaolinite, smectite	3.260	3.038×10^{-5}	97.30	**232.3±5.1**
Sukoró, Rigó-hill	granite, no alteration	orthoclase	9.747	8.9088×10^{-5}	89.60	**220.9±6.7**

lead isotope data obtained for galena are as follows: $^{206}Pb/^{204}Pb = 18.278–18.363$, $^{207}Pb/^{204}Pb = 15.622–15.690$ and $^{208}Pb/^{204}Pb = 38.439–38.587$ (Table 3). Lead isotope ratios for galena from the Szabadbattyán Block are slightly higher: $^{206}Pb/^{204}Pb = 18.286–18.348$, $^{207}Pb/^{204}Pb = 15.667–15.736$ and $^{208}Pb/^{204}Pb = 38.552–38.781$. However, these data are marginally different to those from the Velence Mts only, taking the analytical uncertainties into consideration. The results for calcite and fluorite from the base-metal-fluorite veins of the Velence Mts are close to, but typically slightly more evolved than those for galena of the same veins (Table 3).

Thus, the isotope data from the two areas form a tight cluster and, besides, one can note a tendency towards a linear array (Table 3).

When treated together, the galena data from the two areas yield μ values of 9.8–10.3 (Table 3), following the S-K model (Stacey & Kramers 1975). This is higher than the average crustal value ($\mu_2 = 9.74$), and a dominant upper crustal source for ore lead is also indicated by the plumbotectonic model of Zartman & Doe (1981). Model ages, based on the $^{206}Pb/^{204}Pb$ and $^{207}Pb/^{204}Pb$ data for the combined galena data set are quite consistent at around 300 Ma when the Cumming & Richards (1975) model is applied, whereas S-K model ages vary considerably (286–477 Ma).

XRPD results and clay mineralogy

XRPD analyses were carried out on the clay mineral assemblage of the argillic alteration halo of the granite-hosted hydrothermal base-metal-fluorite veins in the Velence Mts. Argillic alteration zones without base metal mineralization along NE–SW trending faults were also studied. The colour of alteration zones changes from the fresh granite towards the central part of the alteration zones: the central parts are more greenish, while the lateral parts of the alteration are dominated by white clay minerals (Fig. 4a). According to the XRPD studies the green coloured clay is dioctahedral smectite with calcium and/or magnesium in the interlayer space. The basal reflection is shifted from 15 Å to 12.6 Å after potassium saturation, indicating the low-layer charge of the smectite. The Greene-Kelly test indicates that this charge arises from isomorphic substitution in the octahedral sheet (Greene-Kelly 1953). These results show that the smectite is a low charged montmorillonite. Besides montmorillonite, illite/montmorillonite, white coloured mixed layer clay mineral containing 15–20 % illite, pure illite and kaolinite are also present. Illite crystallinity has been checked by combined XRPD and IR spectroscopic analyses (Benkó 2008) and both methods have indicated a well-crystallized R3-type illite based on the classification scheme of Środoń (1984).

K–Ar radiometric ages

K/Ar ages for illite ($n = 4$) are between 209.8 and 232.3 Ma, with individual errors in the order of ±10 Ma, or less. One K-feldspar from the relatively fresh granite (sample 6620) yielded an age of 220.9 Ma, which is comparable to the ages of the illite (Table 4, Fig. 6).

Discussion

Our studies suggest that petrographic, fluid inclusion and isotope data do not support old genetic models stressing that base-metal-fluorite mineralization in the Velence Mts can be related to the formation of the granite.

Nature of the ore-forming fluids

The petrography of fluid inclusions in the Velence Mts suggest trapping from a homogeneous parental fluid, there-

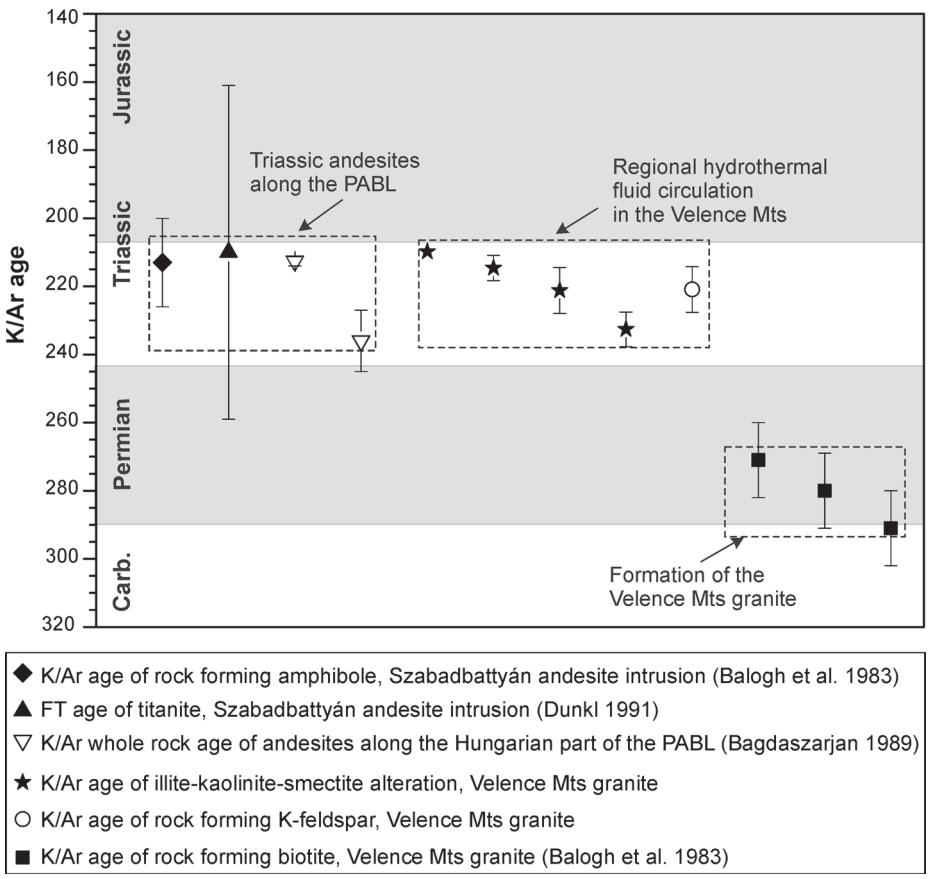

Fig. 6. Radiometric age dates measured on different mineral fractions in the Velence Mts and at the Szabadbattyán Block.

fore the measured homogenization temperatures are only minimum estimates of the trapping conditions. True trapping temperatures and pressures can be obtained only by pressure correction using an independent thermometer.

Field evidence combined by the XRPD results indicates that illite (white) was the first phase to form due to fluid/rock interaction, followed by kaolinite (white) and smectite (green) as gradual opening of the faults proceeds. In hydrothermal systems clay mineral assemblages are useful for temperature estimation (Reyes 1990; Hedenquist & Lowenstern 1994; Parry & Jasumback 2002). Pure illite forms above 220–250 °C, while kaolinite and smectite form below 180 (200) °C. Consequently, it may be suggested that mineralization in the Velence Mts started at temperatures above 250 °C, resulting in illite alteration, and with gradual cooling of the fluids below 200 °C there was a formation of kaolinite and smectite. Sulphur isotope analyses on syngenetic galena-sphalerite mineral pairs also provided temperatures around 230–250 °C (Benkó 2008), which support the view that the maximum temperature of the hydrothermal system could be around 250 °C.

Fluid inclusions with $NaCl-H_2O$ and $CaCl_2-H_2O$ model compositions are simultaneously present as primary objects in the hydrothermal quartz and fluorite in the Velence Mts and as secondary inclusions in the rock-forming quartz of the granite. In spite of the compositional differences, their homogenization temperature distributions in all outcrops are the same and the number of their FIP increases towards the alteration zones. If we assume that these inclusions relate to the cool-

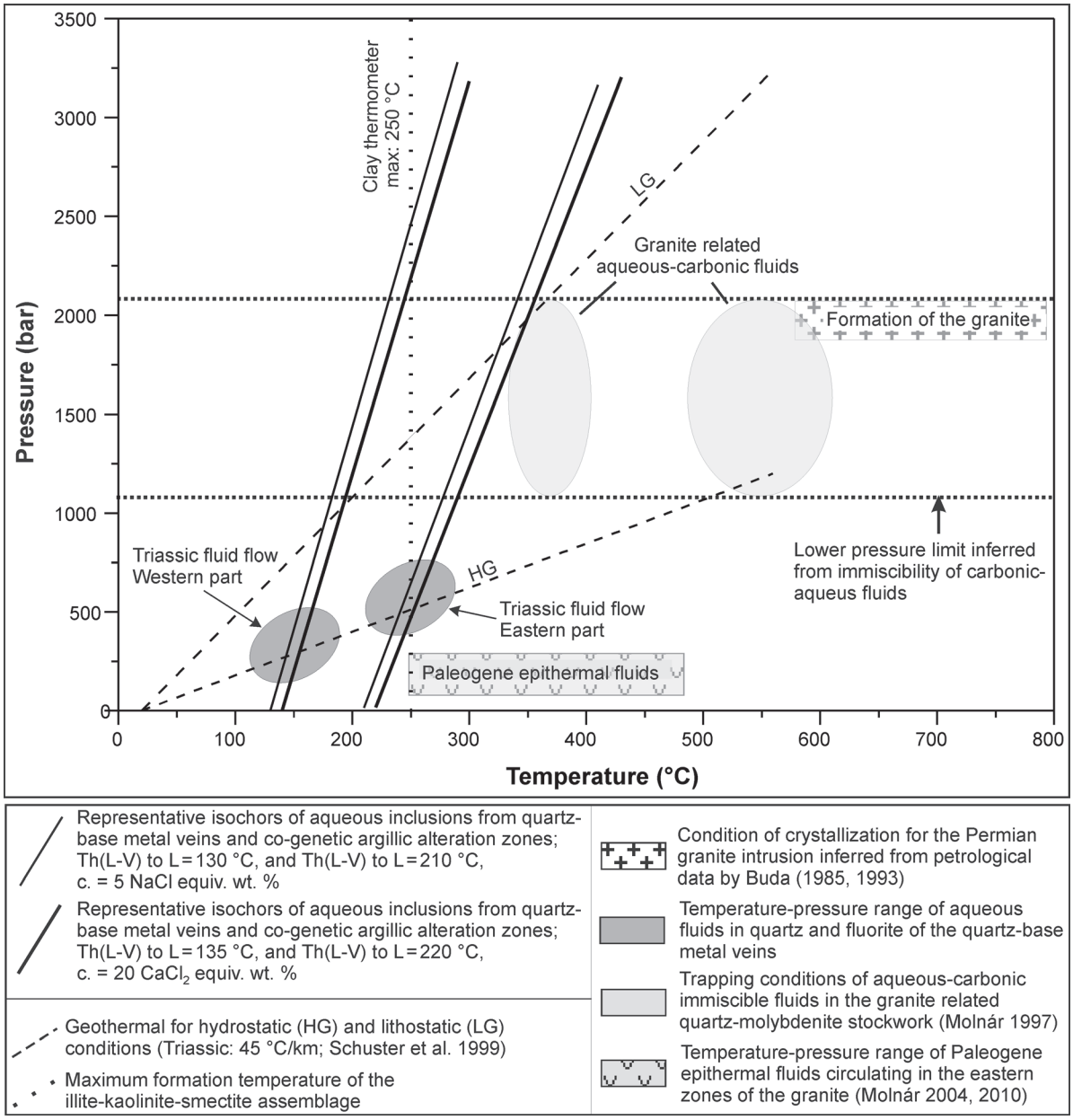

Fig. 7. Temperature–pressure conditions of fluid inclusion entrapment in the Triassic and Alpine hydrothermal systems of the Velence Mts. Isochors were calculated on the basis of equations of Zhang & Frantz (1987). **c.** — concentration.

ing of the granite which crystallized at 2 kbar (Buda 1993; Fig. 7), the isochores for the low homogenization temperature (Th ~ 90–120 °C) inclusions should have crossed the 2 kbar isobar at 150–220 °C. This low temperature at 6–8 km, according to the 2 kbar pressure, assumes a very low geothermal gradient (20 °C/km). In the case of a cooling granite body, a higher temperature than the average (35 °C/km) geothermal gradient is expected. Therefore the observed fluid inclusion features is difficult to relate to the postmagmatic-hydrothermal system of the granite as it was suggested by Jantsky (1957).

The estimated geothermal gradient during the Triassic was 45 °C/km (Schuster et al. 1999). Intersecting the Triassic (45 °C/km) geotherm calculated for hydrostatic and lithostatic conditions with the isochors of the fluid inclusions from the eastern block of the granite, the obtained pressures are between 400 and 1200 bars. Intersecting the isochors of the higher homogenization temperature group (eastern block; 210–220 °C) with the 250 °C isotherm (which is the assumed maximum temperature for illite crystallization; Reyes 1990; Hedenquist & Lowenstern 1994; Parry & Jasumback 2002), results in pressures around 400 bar (Fig. 7). This pressure is lower than the estimated pressure at the time of the formation of the granite, higher than the pressure range for the Paleogene hydrothermal system (30–280 bar, Molnár 1996; Fig. 7) and equivalent to the pressure calculated by the interception of the isochors and the Triassic (hydrostatic) geotherms (Fig. 7). Therefore it is assumed that the pressure conditions during the fluid circulation could be near-hydrostatic. Differences in homogenization temperatures between the eastern and the western block of the granite can be explained by post-hydrothermal tectonic activity of the Pákozd Line (Benkó 2008).

In petrography the fluid inclusion assemblages associated with the Paleogene intrusive-volcanic activity in the eastern part of the Velence Mts are significantly different from the fluid inclusion assemblages in the western part of the granite (e.g. boiling of low-, and high-salinity fluids with temperatures between 250 °C and 450 °C; Molnár 2004; Fig. 7), therefore we proceed to explore the possibility that all of the studied fluid inclusion populations are linked to a third fluid flow event independent from those in the Paleogene and Permian.

Fluid inclusion data for Alpine-type epigenetic lead-zinc ore deposits hosted by Triassic carbonate rocks along the PABL in the Drau Range (Mežica, Bleiberg) are similar to our results for the mineralization of the Velence Mts (Fig. 8). The Alpine-type epigenetic Pb-Zn ore deposit is a subtype of the carbonate hosted stratabound Pb-Zn mineralizations. The mineralization is epigenetic, hosted by Ladinian–Carnian limestones in the Eastern and Southern Alps. The ores have simple mineralogy, containing galena, sphalerite, pyrite and marcasite. Zeeh et al. (1998) reported that the temperature of the hydrothermal fluids of the first ore phase ranged between 122 °C and 159 °C (Phase I; Fig. 9). In their study, the salinity of the early ore forming fluids was 8–12 NaCl equiv. wt. % in sphalerite and 15–19 NaCl equiv. wt. % in saddle dolomite. The salinity of the late hydrothermal phase was higher as indicated by the data from fluorite (18–21 NaCl equiv. wt. %). A similar mixing of low- and high salinity fluids during ore formation in the Velence Mts was first suggested by Molnár (1996). Maintaining the concept of a mixing model including two types of fluids we postulate that fluid mixing may have played a significant role in ore formation.

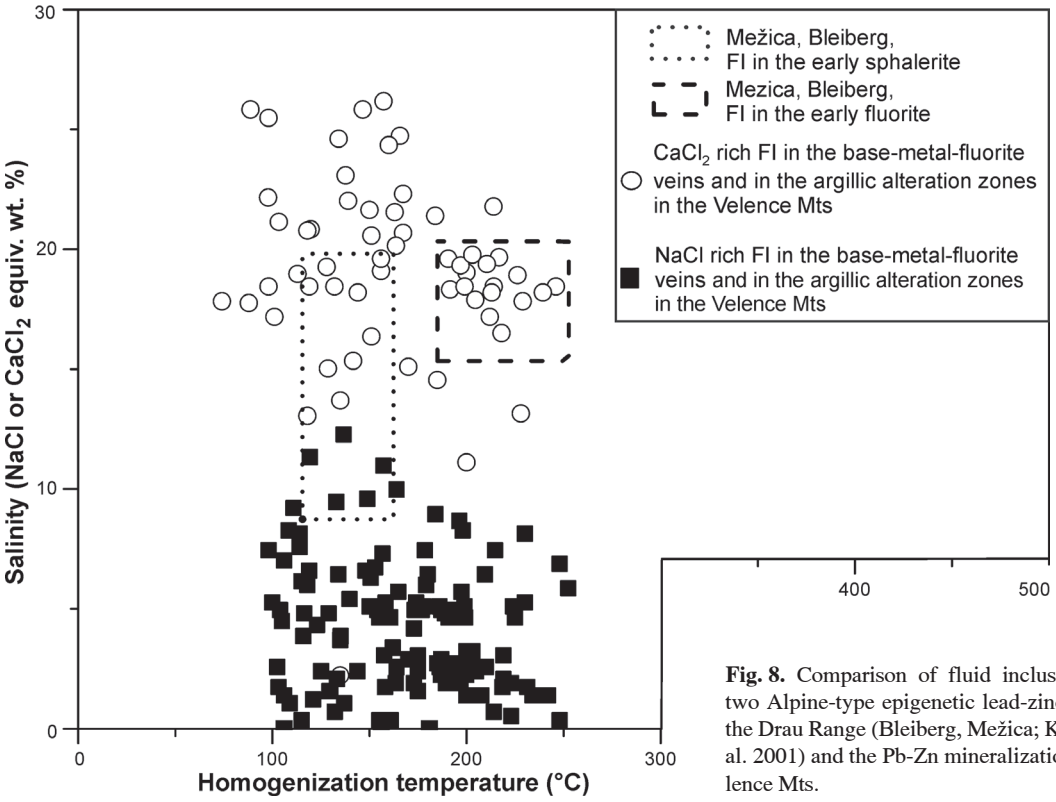

Fig. 8. Comparison of fluid inclusion data for two Alpine-type epigenetic lead-zinc deposits in the Drau Range (Bleiberg, Mežica; Kuhlemann et al. 2001) and the Pb-Zn mineralization of the Velence Mts.

Sources of Pb in the veins

The lead isotope ratios in the base-metal-fluorite veins of the Velence Mts and the Szabadbattyán Block essentially overlap (Fig. 9a,b) with the data for galena from Alpine-type epigenetic Pb-Zn mineralizations along the PABL (Bleiberg, Mežica, Salafossa, Raibl, Gorno (Figs. 1 and 11). Köppel & Schroll (1988) proved the importance of early Paleozoic high-grade metamorphic crystalline basement rocks (gneiss, amphibolite, micaschist) as sources of metals in the Alpine-type lead-zinc deposits. High-grade metamorphic rocks are not known in the currently studied areas, but pebbles of such rocks were documented in a late Variscan molass formation, located close to the reconstructed pre-tectonic site (cf. the Carboniferous conglomerate in Fig. 10c).

It is therefore possible that the metals in the investigated deposits of the Pannonian Basin were also derived from a range of rocks, including spatially associated magmatic rocks (the host rock granite in the Velence Mts and the andesite dykes at Szabadbattyán), the underlying sedimentary rocks and the deeply situated metamorphic basement. Interestingly, despite the difference in host rock character (Permian granite and Devonian limestone, respectively), the ore lead signatures at the Velence Mts and at the Szabadbattyán Block are more or less identical (Fig. 9a,b). This suggests that the host limestone in the Szabadbattyán Block did not act as a major source of lead, and it is more likely that a range of deep-seated rocks provided the metals.

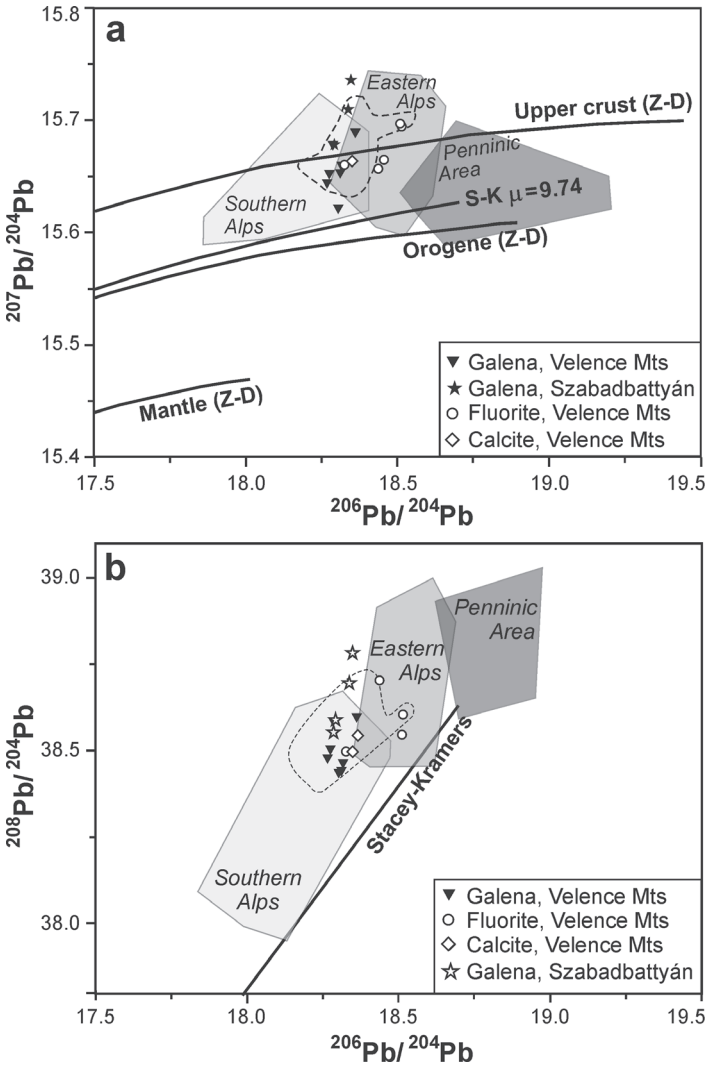

Fig. 9. Lead isotope evolution diagrams (**a** — $^{207}Pb/^{204}Pb$–^{206}Pb–^{204}Pb, **b** — $^{208}Pb/^{204}Pb$–$^{206}Pb/^{204}Pb$) with growth curves according to Zartman & Doe (1981) (Z–D) and Stacey & Kramers (1975). The shaded boxes represent whole rock Pb isotope data of the three main tectonic units of the Alps (Köppel & Schroll 1988). The field bordered by dashed line represents lead isotope data from galena of Alpine-type Pb-Zn deposits along the PABL (Köppel 1983). Data points represent lead isotope data from the Velence Mts and the Szabadbattyán Block measured in galena and fluorite.

Radiometric age constraints and age correlations with adjoining areas

The age of the host granite in the Velence Mts is 280–290 Ma (Buda 1985) as is indicated by the K/Ar, Rb–Sr data for rock-forming biotite. The K/Ar blocking temperature of pure illite is around 250 °C (Clauer & Chaudhuri 1995). Hence, it seems plausible that the measured K/Ar age data from pure illite from the argillic alteration zones around the base-metal-fluorite veins of the Velence Mts represent the true age of the hydrothermal circulation. As the obtained K/Ar ages of 210–230 Ma almost overlap within analytical error, it is possible to establish a Mid-Late Triassic ore-forming event (Fig. 6). K/Ar data for the orthoclase from the western part of the granite body at Velence Mts also provide support for a Mid-Late Triassic thermal event. This is based on the fact that the blocking temperature of K-feldspar is around 160 °C (Harrison et al. 1979), and therefore the K/Ar ages of feldspars either represent the time of cooling of the rock below 160 °C (Faure 1977; Richards & Noble 1998) or the post-emplacement history involving other events when the temperature of the rock passed the 160 °C isograd for the last time. Following this, we anticipate that the 221 Ma age of the rock forming fresh orthoclase represents a re-set age which is due to a regional heating of the granite body above 160 °C in Triassic times. Evidently, the inferred Triassic hydrothermal alteration was not related in age to the Carboniferous, magmatism (host granite), Cretaceous lamprophyre dykes or to the Paleogene magmatic activity in the easternmost part of the Velence Mts. Therefore, we can rule out any hypothesis (Jantsky 1957; Kaszanitky 1958; Horváth & Ódor 1984) assuming that either of these magmatic events acted as the heat source for the mineralizing fluids.

Triassic magmatic activity in the Velence Mts is not known, but age data for andesite dikes from the Szabadbattyán Block (Balogh et al. 1983; Bagdaszarjan 1989; Dunkl 1991) are equivalent to the obtained K/Ar ages for illite in the Velence Mts. This is exemplified by a 210 ± 4 Ma K/Ar age of whole rock samples of one andesite dyke from Szabadbattyán

(Bagdaszarjan 1989), whereas Balogh et al. (1983), obtained 213 ± 13 Ma for another dyke. Dunkl (1991) established a 214 ± 5 Ma age for titanite from those andesite dykes by the fission track method (Fig. 6). This age agreement between the two mineralized study areas suggests that a presently not identified Triassic magmatic event might have been the driving force for hydrothermal alteration in the Velence Mts. This view is consistent with an active Triassic magmatism along the eastern segment of the PABL (Ferrara & Innocenti 1974). There is evidence that it also extended into the Southern Alps. The eastern part of the Neo-Tethys region is characterized by slightly older magmatism (Haas 2004). Pamić (1984) reported Ladinian magmatic ages in the 216–250 Ma range in the Karawanken, by using a range of isotopic methods (U–Pb, Rb–Sr and K/Ar data), which may be related to the rift phase of the Dinaric part of the Neo-Tethys Ocean. Castellarin et al. (1988) documented Ladinian bimodal magmatites from the Southern Alps. However, on the basis of geochemical data, they emphasized an orogenic origin of the magmas.

It is not the aim of this paper to discuss whether the Ladinian magmatic rocks in both the Alpine region and along the PABL have a rift or an orogenic origin. Still, as a general theory (cf. Haas 2004), we prefer the rift origin and we connect the Ladinian hydrothermal circulation in the Velence Mts and the Szabadbattyán region to the contemporaneous rift events in the Neo-Tethys Ocean.

Model of formation of lead-zinc deposits in the Pannonian Basin and their possible genetic link to the Alpine-type epigenetic mineralizations

Comparison of the studied deposit and the Alpine deposits is summarized in Table 5.

There are striking similarities between the granite-hosted deposit in the Velence Mts and certain deposits (Mežiča, Bleiberg, Salafossa, Gorno, etc.) in the Alps along the PABL (Fig. 10a,b, Table 5), especially regarding fluid inclusion and lead isotope signatures. However, the host rock of the

Table 5: Comparison of geochemical, fluid inclusion and mineralogical characteristics of the studied (Szabadbattyán and Velence Mts) and other base-metal and fluorite mineralizations along the PABL (Bolzao granodiorite, Alpine-type epigenetic lead-zinc mineralizations).

	Bozen porphyry	**Epigenetic mineralizations along the PABL**		**Mineralizations along the PABL in the Pannonian Basin**	
	Vein type F mineralization	*South of the PABL* (Raibl-Salafossa)	*North of the PABL* (Mežica-Bleiberg)	Velence Mts	Szabadbattyán
Host rock	metamorphic basement, Bozen quartz porphyry, (275–285 Ma) granodiorite (222 Ma)	dolomite, Buchenstein tuff (Anisian–Ladinian)	Wetterstein dolomite/ Raibl beds (Carnian)	Early Permian monzogranite	Devonian limestone
Style of mineralization	vein-type	stratiform (linked to faults) columnar orebodies vein-type	stratabound vein-type, breccia	vein-type, brecciated	metasomatic replacement, karst filling, vein type
Ore minerals	fluorite	sphalerite, galena accessoric: *sulphosalts, pyrrhotite, chalcopyrite (?)*	sphalerite, galena, accessoric: *marcasite, pyrite, melnikovite*	galenite, sphalerite accesoric: *pyrite, antimonite, chalcopyrite, fahlore, chalcocite*	galenite, sphalerite accesoric: *bournonite, native Ag tetrahedrite, chalcopyrite*
Gangue and alteration minerals of the host rock	quartz, barite, calcite, siderite, dolomite	dolomite, barite, quartz, acid feldspar, clay minerals	fluorite, quartz, calcite, dolomite, barite	fluorite, calcite, illite, kaolinite, smectite, barite	calcite, quartz
Ore texture	cockade, rhytmic banding, syngenetic brecciation	colloform, vein filling, cavity fills	bedded colloform, diagenetic replacements, deformation breccias	banded, cocade, brecciated	metasomatic replacement, karst filling, subordinately vein-type
Geochemistry	no data	Pb, Zn, Cd, Tl, As, Ge	Pb, Zn, Cd, Tl, As, Ge 470 ppm Cu at Mežica in sphalerite	Pb, Zn, Cu, Cd, Ag, Au, Fe, As, Sb	Pb, Zn, Ag, Cu, As, Sb
Ore forming fluids	230→170 °C 20→7 NaCl equiv. wt. % cooling and concentration of hydrothermal fluids	no data	200–122 °C 21–18 NaCl equiv wt. % 12–8 NaCl equiv wt. % (fluorite and sphalerite)	80–220 °C 1–28 NaCl or NaCl+$CaCl_2$ equiw. wt. %	no data
Pb isotope ratios $^{206}Pb/^{204}Pb$ $^{207}Pb/^{204}Pb$ $^{208}Pb/^{204}Pb$	no data	(average at Raibl) 18.386 ± 0.006 15.685 ± 0.004 38.621 ± 0.017	(average at Mežica) 18.362 ± 0.012 15.669 ± 0.010 38.532 ± 0.025	18.268–18.515 15.622–16.658 38.439–38.770	18.286–18.348 15.667–16.736 38.552–38.781
Sulfur isotope	no data	(average at Raibl) –6.43 to –25.60	(average at Mežica) –1.7 to –20.93	–1.48 to –2.70	no data
Age of mineralization	Permian–Late Triassic	Mid-Triassic	Late–Triassic	Mid-Late Triassic K/Ar age of illite: 209–232 Ma	no data
Source and transport of metals	Paleozoic basement rocks formational fluids, regional fluid flow	Leaching of basement rocks, during regional fluid flow and/or volcanic activity		Paleozoic basement rocks formational fluids, regional fluid flow	
References	Hein et al. 1990	Brigo et al. 1977; Köppel 1983; Schroll & Pak 1983	Brigo et al. 1977; Köppel 1983; Schroll & Pak 1983; Zeeh et al. 1998; Kuhlemann et al. 2001	Molnár 2002; Gyalog & Horváth 2004	Kiss 2003

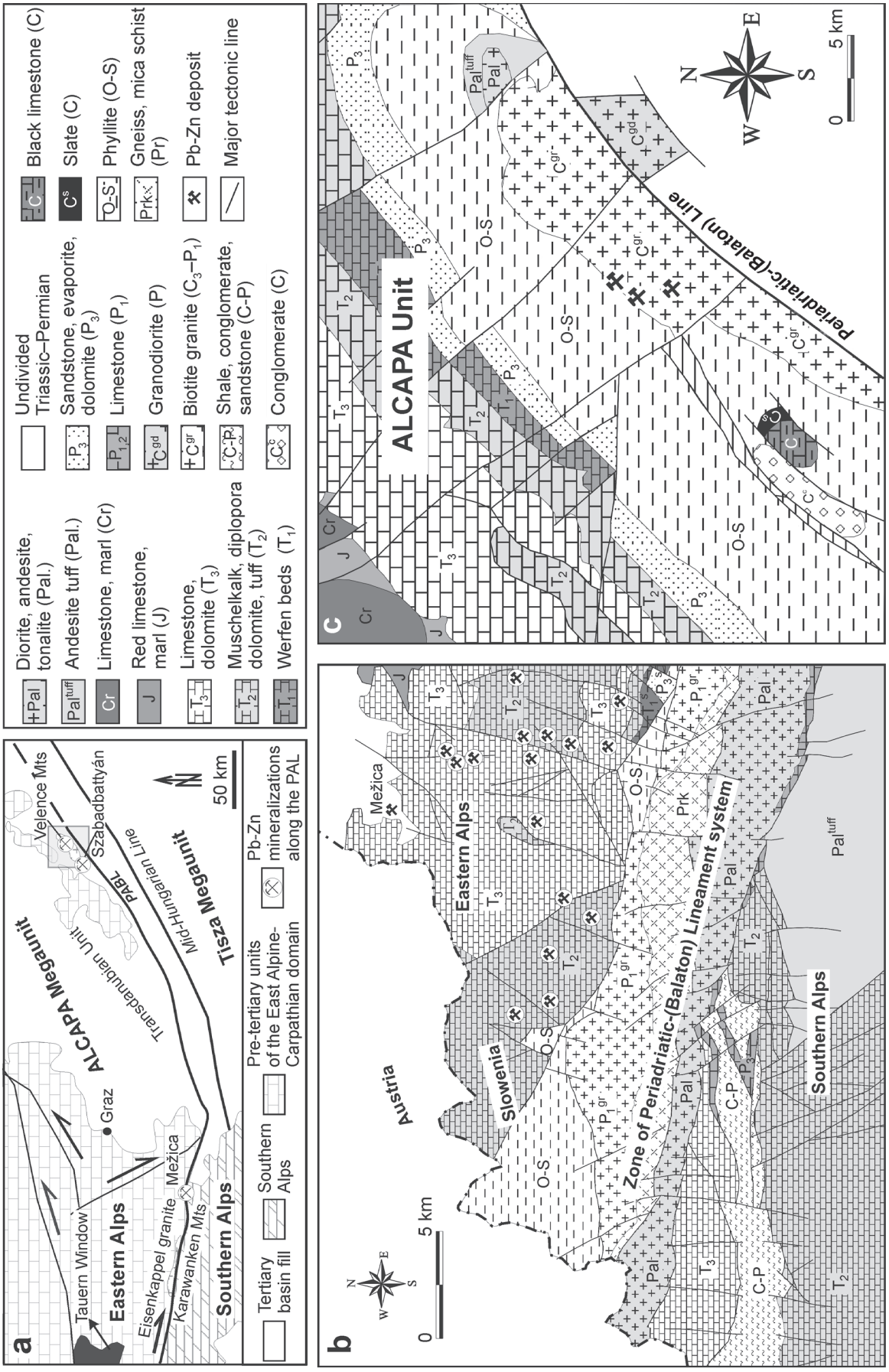

Fig. 10. a — Regional geology of the SE part of the Alcapa Megaunit and the eastern part of the Eastern and Southern Alps after Kázmér & Kovács (1985). The Alcapa Megaunit escaped during the Late Paleogene–Early Neogene from the collision zone of the Eastern Alps and Southern Alps along the dextral PABL; **b** — Pb-Zn deposits along the PABL in the eastern segment of the Eastern Alps (Bauer 1985); **c** — Pb–Zn in deposits along the PABL in the Pannonian basin (Szabadbattyán Block and Velence Mts after Dudko 1999). The similar geology in the broader vicinity of the Pb–Zn deposits suggests that these deposits could be spatially in contact prior to the escape of the Alcapa Megaunit from the Alpine collision zone.

Alpine-type epigenetic lead-zinc deposits in the Alps is mainly Triassic limestone (e.g. Raibl beds) and the ores occur as stratabound bodies, whereas mineralization in the Velence Mts is characteristically vein-type, hosted by granite. Mineralization in the Alpine deposits often occurs as matrix of tectonic breccias, but also forms fissure filling, karst filling or fault-related epigenetic ore bodies (Brigo et al. 1977). This suggests that the diagenetic process and the carbonate host rock are not truly decisive factors for governing ore deposition, and mineralization can occur in very different forms and in different type of rocks.

Also, the timing aspect is important when a potential genetic link is tested between different ores. Observations presented in this paper argue for an epigenetic, Mid-, Late-Triassic ore-forming event in the Velence Mts and the Szabadbattyán Block (209–232 Ma). Epigenetic lead-zinc deposits north of the PABL occur in the Late–Triassic (Carnian — 228–216 Ma; Brigo et al. 1977).

Another candidate for comparison along the PABL is the Brixen (Bolzano) granodiorite (Fig. 1), which is the host of vein type quartz-fluorite mineralization. Age, geochemical, and genetic similarities of the two host crystalline formations have been established by Buda et al. (2004). Age, texture and fluid inclusion properties of the two mineralizations in the Velence Mts and in the Szabadbattyán Block also show several striking similarities (Table 5). On the basis of the characteristics of the Bolzano mineralization, Hein et al. (1990) connected the formation of the quartz-fluorite veins to a large-scale fluid flow system and excluded the possible role of magmatism as a driving force of fluid flow. In his model, fluorine originated from the sedimentary basement rocks. Based on the fluorine anomalies in the carbonate-hosted lead-zinc deposits along the PABL, he proposed a genetic link between the granite hosted quartz-fluorite veins and the lead-zinc deposits. Regarding the large distance between Bolzano granite and the studied deposits (~600 km along the PABL) it is not necessarily stated that the two crystalline formations formed an identical unit. However, if the Velence Mts are interpreted as a tectonic megamelange along the PABL the former spatial relationship of the two rock units cannot be excluded.

In our model a rift related regional fluid flow was initiated by the time of the Mid Triassic. The heat source of the fluid convection could be the attenuated and heated continental crust but locally magma intrusions may also have played a significant role. Ca-rich, high-salinity formational fluids migrating in the basement metamorphic and sedimentary rocks leached base metals. Mixing with low-salinity fluids and cooling decreased their transfer capacity and base metals precipitated in some tectonic zones (Fig. 11). Consequently, base-metal veins in the Velence Mts represent the relatively deep channels of the fluid flow, whereas epigenetic deposits in the Alps are the uppermost, discharge part of a similar hydrothermal system.

The spatial relationship between the different levels of the hydrothermal convection system is not obvious at first sight. However several authors (Géczy 1984; Dulai 1990; Vörös 1993; Csontos 1995; Haas et al. 1995; Ebner et al. 1998; Márton & Fodor 2003) proved that the Transdanubian Mountain Range escaped 450–500 km east from the Alpine collision zone during the Late Paleogene–Early Neogene. Accordingly, in the Triassic, in its original position the Velence

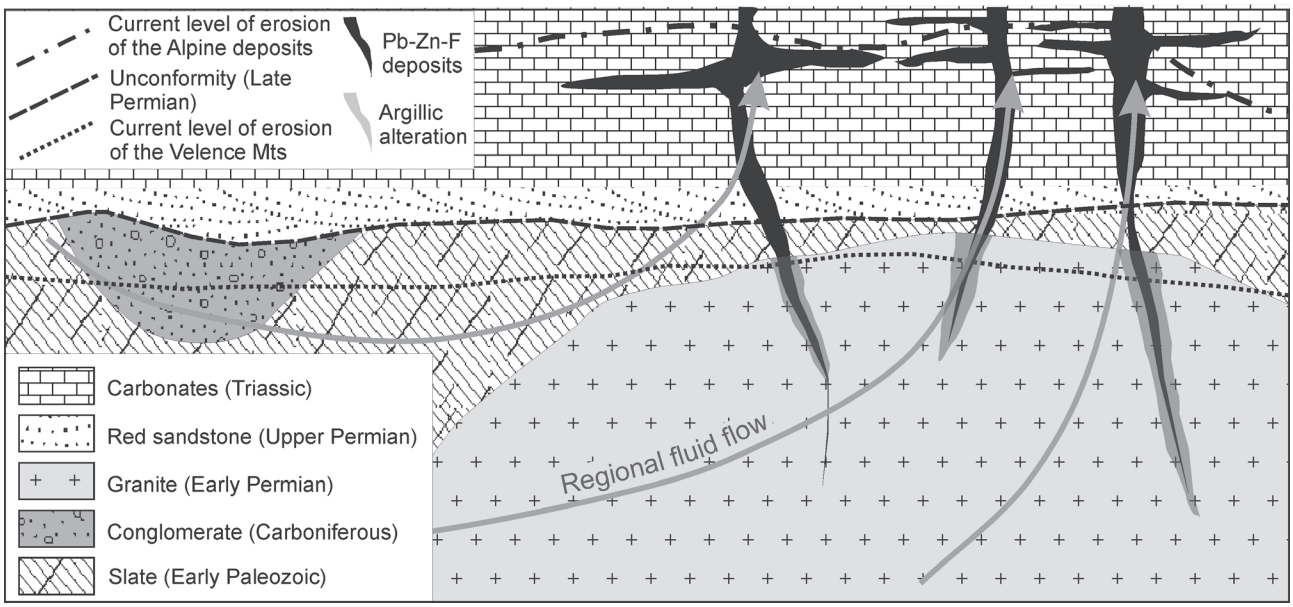

Fig. 11. Proposed genetic model of lead-zinc mineralization in the Velence Mts and its possible connection to the Alpine-type epigenetic lead-zinc mineralization, without scale. Base-metal-fluorite mineralization in the Velence Mts represents a deep conduit part of the hydrothermal system. During ascent and cooling of hydrothermal fluids, fissure filling and brecciated lead-zinc ore formed in Triassic limestones along the PABL. Carbonate hosted Alpine-type epigenetic lead-zinc deposits formed at the discharge site of the convection system. Due to the different tectonic histories during the Alpine orogeny epoch, shallow levels of the system are preserved in the Alps, whereas the deeper part of the system is exposed in the central part of the Pannonian Basin.

Mts formed the basement of the carbonaceous sedimentary formations that are now the host of the stratiform-stratabound epigenetic deposits. Due to the intense orogenic processes during the Alpine orogeny in the Createceous some parts of the system were lifted up more intensively and eroded (Velence Mts, Szabadbattyán on the southern flank of the syncline of the Transdanubian Mountain Range) while other parts were not exhumed and eroded (Alpine-type epigenetic lead-zinc deposits).

Later, as a result of the eastward extrusion of the Alcapa Megaunit from the Alpine collision zone, the two levels of the former hydrothermal system were farther displaced.

Carbonaceous rocks similar to the host of the Alpine deposits far north from the PABL are widely known in the Transdanubian Mountain Range. Except for a few indications, no mineralization has been found yet in these rocks. This implies that the PABL as a major fluid flow channel had a particular role in the formation of the various lead-zinc deposits.

Summary and conclusions

Clay mineralogy, K/Ar radiometric ages, lead isotope and fluid inclusion studies have been carried out on the vein type and metasomatic base-metal-fluorite mineralization of the Paleozoic basement units of the Pannonian Basin in the Velence Mts and the Szabadbattyán Block in order to establish a model for their origin.

The maximum temperature of the hydrothermal fluid flow was around 250 °C according to the clay mineral studies. The fluids then gradually cooled during the hydrothermal fluid flow to below 200 °C. Formation of the base-metal-fluorite mineralization is the result of the mixing of low salinity (0–12 NaCl equiv. wt. %) and high salinity (10–26 $CaCl_2$ equiv. wt. %) formational brines. Our studies on fluid inclusions and clay gangue minerals indicate that the temperature (130–240 °C) and pressure conditions (400–500 bar) during ore formation were different from the magmatic–postmagmatic system for the Permian granite intrusion (550–690 °C; 2 kbar) and the Paleogene fluid flow (240–480 °C; 30–280 bars).

Lead isotope data (Velence Mts: $^{206}Pb/^{204}Pb = 18.278–18.363$, $^{207}Pb/^{204}Pb = 15.622–15.690$ and $^{208}Pb/^{204}Pb = 38.439–38.587$ and Szabadbattyán: $^{206}Pb/^{204}Pb = 18.286–18.348$, $^{207}Pb/^{204}Pb = 15.667–15.736$ and $^{208}Pb/^{204}Pb = 38.552–38.781$) demonstrate a common isotope pattern for the two studied mineralizations and the obtained results are also in concordance with data for Alpine-type epigenetic lead-zinc deposits. Magmatic rocks and basement metamorphic rocks, carrying an upper crustal signature, probably supplied a major part of the lead contained in the ores.

K/Ar radiometric age dating (208–232 Ma) suggests a Mid- to Late-Triassic age of the mineralization and related regional heating of the granite. Thus our results give no support to earlier hypotheses, including ore formation related to Carboniferous, Cretaceous and Paleogene magmatism.

Several lines of presented evidence suggest a genetic relationship between the two studied mineralization of the Pannonian Basin and other, Alpine-type epigenetic lead-zinc deposits along the PABL, in the Southern and Eastern Alps. A tectonic reconstruction suggests a direct spatial relationship to the deposits along the PABL in the Southern and Eastern Alps. We propose that the two described mineralizations in the Pannonian basin are deep feeder channels of a regional fluid flow system that occasionally discharged to form shallow epigenetic Pb–Zn mineralizations. The latter are now eroded away, if they were ever present in the study areas.

Acknowledgments: The measurements were supported by the Synthesys (SE-TAF-3772) program of the EU. The authors are particularly grateful to the editor Pavel Uher and the reviewers, Peter Koděra and Sándor Szakáll for their detailed review of the manuscript. Their suggestions and constructive criticism of the earlier manuscript resulted in major improvements to the final article.

References

Bagdaszarjan G.P. 1989: Radiometric age dates of samples from the Velence Mts — Manuscript. *Geol. Inst. Hung.*, Budapest.

Bajnóczi B. 2003: Palaeogene hydrothermal processes in the Velence Mountains, Hungary. *Unpublished PhD Thesis, ELTE University,* Budapest, 1–116.

Bajnóczi B., Molnár F., Maeda K., Nagy G. & Vennemann T. 2002: Mineralogy and genesis of primary alunites from epithermal systems of Hungary. *Acta Geol. Hung.* 45, 1, 101–118.

Balogh K. 1985: Principles, application of the K-Ar age dating method, and data interpretation. *Mineral. Geochem. Rev.*, Budapest, 1–49.

Balogh K., Árva-Sós E. & Buda Gy. 1983: Chronology of granitoid and metamorphic rocks of Transdanubia (Hungary). *Ann. Inst. Geol. Geofiz.* 61, 259–364.

Bauer F.K. 1985: Geological Map of the Karawanken 1:25,000, Westteil. *Geol. Bundesanst.,* Wien.

Benedek K. 2002: Palaeogene igneous activity along the easternmost segment of the Periadriatic–Balaton Lineament. *Acta. Geol. Hung.* 45, 4, 359–371.

Benedek K., Pécskay Z., Szabó Cs., Jósfai J. & Németh T. 2004: Palaeogene igneous rocks in the Zala basin (Western Hungary): Link to the Palaeogene magmatic activity along the Periadriatic lineament. *Geol. Carpathica* 55, 1, 43–50.

Benkó Zs. 2008: Reconstruction of multi-phase fluid flow history and tectonic evolution in a Variscan granite intrusion (Velence Mts., Hungary). *Unpublished PhD Thesis, ELTE University*, Budapest, 1–162.

Benkó Zs. & Molnár F. 2004: Application of studies on fluid inclusion planes for evaluation of structural control on Variscan and Alpine fluid mobilization processes in the monzogranite intrusion of the Velence Mts., (W-Hungary). *Acta Mineral. Petrogr.,* Szeged 45, 1, 123–131.

Benkó Zs., Molnár F. & Lespinasse M. 2008: Application of studies on fluid inclusion planes and fracture systems in reconstruction of fracturing history of granitoid rocks I.: introduction to methods and implication for fluid-mobilization events in the Velence Mts. *Bull. Hung. Geol. Soc.* 138, 3, 229–246.

Benkó Zs., Molnár F., Pécskay Z., Németh T. & Lespinasse M. 2012: The interplay of the Palaeogene magmatic-hydrohermal fluid flow on a Variscan granite intrusion. age and formation of the barite vein at Sukoró, Velence Mts, W-Hungary. *Bull. Hung. Geol. Soc.* 142, 1, 45–58.

Bodnar R.J. 1993: Revised equation and table for determining the

freezing point depression of H_2O–NaCl solutions. *Geochim. Cosmochim. Acta* 57, 683–684.

Brigo L., Kostelka L., Omenetto P., Schneider H.J., Schroll E., Schulz O. & Štrucl I. 1977: Comparative reflections on four Alpine lead–zinc deposits. In: Klemm D.D. & Schneider H.J. (Eds.): Time- and strata-bound ore deposits. *Springer*, Berlin, 273–294.

Broska I. & Uher P. 2000: Whole-rock chemistry and genetic typology of the West-Carpathian Variscan granites. *Geol. Carpathica* 52, 79–90.

Buda Gy. 1985: Origin of collision-type Variscan granitoids in Hungary, West Carpathian and Central Bohemian Pluton. *Unpublished PhD. Thesis*, Budapest, 1–148.

Buda Gy. 1993: Enclaves and fayalite bearing pegmatitic "nests" in the upper part of the granite intrusion of the Velence Mts, W-Hungary. *Geol. Carpathica* 44, 3, 143–153.

Buda Gy., Koller F. & Ulrych J. 2004: Petrochemistry of Variscan granitoids of Central Europe: Correlation of Variscan granitoids of the Tisia and Pelsonia terranes with granitoids of the Moldanubicum, Western Carpathians and Southern Alps. A review: part I. *Acta Geol. Hung.* 47, 2–3, 117–138.

Castellarin A., Lucchini F., Rossi P.L., Selli L. & Simboli G. 1988: The Middle Triassic magmatic–tectonic arc development in the Southern Alps. *Tectonophysics* 146, 79–89.

Clauer N. & Chaudhuri S. 1995: Clays in crustal environments. *Springer Verlag*, Berlin, 1–369.

Cumming G.L. & Richards J.R. 1975: Ore lead isotope ratios in a continuously changing Earth. *Earth Planet. Sci. Lett.* 28, 155–171.

Csontos L. 1995: Tertiary tectonic evolution of the Intra-Carpathian area: a review. *Acta Vulcanol.* 7, 1–13.

Csontos L. & Vörös A. 2004: Mesozoic plate tectonic reconstruction of the Carpathian region. *Palaeogeogr. Palaeoclimatol. Palaeoecol.* 210, 1–56.

Csontos L., Nagymarosy A., Horváth F. & Kováč M. 1992: Cenozoic evolution of the Intra-Carpathian area: a model. *Tectonophysics* 208, 221–241.

Darida-Tichy M. 1987: Paleogene andesite volcanism and associated rock alteration (Velence Mountains, Hungary). *Geol. Carpathica* 38, 1, 19–34.

DeIgnacio S.J., Munoz M., Sagredo J., Fernandes-Santin S. & Johansson Å. 2006: Isotope geochemistry and FOZO mantle component of the alkaline–carbonatitic association of Fuerteventura, Canary Islands, Spain. *Chem. Geol.* 232, 99–113.

Dudko A. 1999: Geological map of pre-Sarmatian surface of the Balatonfő-Velence Area. In: Gyalog L. & Horváth I. 2004 (Eds.): Geology of the Velence Hills and the Balatonfő. *Hung. Geol. Inst.* Budapest.

Dulai A. 1990: The Lower Sinemurian (Jurassic) brachiopod fauna of the Lókút Hill (Bakony Mts., Hungary). Preliminary results. *Ann. Hist.–Natur. Mus. Nat. Hung.* 82, 25–37.

Dunkl I. 1991: Fission track dating of tuffaceous Eocene Formations of the north Bakony Mountains (Transdanubia, Hungary). *Acta Geol. Hung.* 33, 1–4, 13–30.

Dunkl I., Horváth I. & Józsa S. 2003: Andesite dykes and skarn formations of the Szár Hill, Polgárdi, Hungary. *Top. Miner. Hung.* 8, 55–86.

Ebner F., Kovács S. & Schönlaub H. 1998: Stratigraphic and facial correlation of the Szendrő–Uppony Paleozoic (NE Hungary) with the Carnic Alps-South Karawanken Mts. and Graz Palaeozoic (Southern Alps and Central Eastern Alps), some paleogeographic implications. *Acta Geol. Hung.* 41, 4, 355–388.

Faure G. 1977: Principles of isotope geology. *John Wiley & Sons,* New York, 1–458.

Ferrara G. & Innocenti F. 1974: Radiometric age evidences of a Triassic thermal event in the Southern Alps. *Geol. Rdsch.* 63, 572–581.

Finger F., Broska I., Haunschmid B., Hraško Ľ., Kohút M., Krenn E., Petrík I., Riegler G. & Uher P. 2003: Electron-microprobe dating of monazites from Western Carpathian basement granitoids: plutonic evidence for an important Permian rifting event subsequent to Variscan crustal anatexis. *Int. J. Earth Sci.* 92, 86–98.

Fodor L., Jelen B., Márton E., Skaberne D., Car J. & Vrabec M. 1998: Miocene–Pliocene tectonic evolution of the Slovenian Periadriatic fault: implications for Alpine-Carpathian extrusion models. *Tectonics* 17, 690–709.

Földvári A. 1952: Lead mineralization and fossiliferous limestone outcrop at Szabadbattyán. *MTA Műsz. Tud. Oszt. Közl.* 5, 1–2, 25–53.

Fülöp J. 1990: Geology of Hungary, Paleozoic. *Hung. Geol. Inst.,* Budapest, 187–202.

Géczy B. 1984: Provincialism of Jurassic ammonites: examples from Hungarian faunas. *Acta Geol. Hung.* 27, 3–4, 379–389.

Greene-Kelly R. 1953: The identification of montmorillonoids in clays. *J. Soil Sci.* 4, 233–237.

Haas J. 2004: Geology of Hungary, Triassic. *ELTE Eötvös Press*, Budapest, 35–74.

Haas J., Kovács S., Krystyn L. & Lein R. 1995: Significance of Late–Permian Triassic zones in terrane reconstructions in the Alpine–North Pannonian domain. *Tectonophysics* 242, 19–40.

Haas J., Mioc P., Pamić J., Tomljenović B., Árkai P., Bérczi-Makk A., Koroknai B., Kovács S. & Felgenhauer E.R. 2000: Complex structural pattern of the Alpine-Dinaridic-Pannonian triple junction. *Int. J. Earth Sci.* 89, 377–389.

Harrison T.M., Armstrong R.L., Naeser C.W. & Harakal J.E. 1979: Geochronology and thermal history of the Coast Plutonic Complex, near Prince Rupert, British Columbia. *Canad. J. Earth Sci.* 16, 400–410.

Hedenquist J.W. & Lowenstern J.B. 1994: The role of magmas in the formation of hydrothermal ore deposits. *Nature* 370, 519–527.

Hein U.F., Lüders P. & Dulski P. 1990: The fluorite mineralization of the Southern Alps: combined application of fluid inclusions and rare earth element (REE) distribution. *Mineral. Mag.* 54, 325–333.

Horváth I. & Ódor L. 1984: Alkaline ultrabasic rocks and associated silicocarbonatites in the NE part of the Transdanubian Mts., Hungary. *Miner. Slovaca* 16, 115–119.

Jantsky B. 1957: Geology of the Velence Mts. *Geol. Hung., Ser. Geol.* 10, 166.

Kaszanitzky F. 1958: Genetic relations of the Pátka–Kőrakás–hegy ore occurrence, Velence Area, North Central Hungary. *Ann. Hist.–Natur. Mus. Nat. Hung.* 50, 9, 19–30.

Kázmér M. & Kovács S. 1985: Permian–Palaeogene paleogeography along the eastern part of the Insubric-Periadriatic Lineament system: evidence for continental escape of the Bakony–Drauzug Unit. *Acta Geol. Hung.* 28, 1–2, 617–648.

Kiss J. 1951: Hydrothermal mineralization on the northern part of the Velence Mts. *Bull. Hung. Geol. Inst. 1953*, 111–127.

Kiss J. 2003: Geology and ore mineralization of the Szár Hill, Polgárdi, Hungary. *Top. Miner. Hung.* 8, 29–54.

Kovács I., Szabó Cs., Bali E., Falus Gy., Benedek K. & Zajacz Z. 2007: Palaeogene–Early Miocene igneous rocks and geodynamics of the Alpine–Carpathian Dinaric region: An integrated approach. *Geol. Soc. Amer., Spec. Pap.* 418, 93–112.

Köppel V. 1983: Summary of lead isotope data from ore deposits of the Eastern and Southern Alps: Some metallogenic and geotectonic implications. In: Schneider H.J. (Ed.): Mineral deposits of the Alpine Epoch in Europe. *Springer*, Berlin–Heidelberg, 162–269.

Köppel V. & Schroll E. 1988: Pb-isotope evidence for the origin of lead in stratabound lead–zinc deposits in Triassic carbonates of the Eastern and Southern Alps. *Mineralium Depos.* 23, 96–103.

Kuhlemann J., Vennemann T., Herlec U., Zeeh S. & Bechstädt T. 2001: Variations of sulfur isotopes, trace element compositions, and cathodoluminesence of Mississippi Valley type lead–zinc ores from the Drau–Range, Eastern Alps (Slovenia–Austria): Implications for ore deposition on a regional versus micro scale. *Econ. Geol.* 96, 1931–1941.

Lespinasse M. & Cathelineau M. 1990: Fluid percolation in a fault zone: a study of fluid inclusion planes in the St. Sylvestre granite, northwest Massiff Central, France. *Tectonophysics* 184, 173–187.

Lespinasse M. & Pecher A. 1986: Microfracturing and regional stress field: a study of preferred orientations of fluid inclusion planes in granite from the Massif Central, France. *Struct. Geol.* 8, 2, 169–180.

Lespinasse M., Désindes L., Fratczak P. & Petrov V. 2005: Microfissural mapping of natural cracks in rocks: Implications for fluid transfers quantification in the crust. *Chem. Geol.* 223, 170–178.

Márton E. & Fodor L. 2003: Tertiary paleomagnetic results and structural analysis from the Transdanubian Range (Hungary): Rotational disintegration of the Alcapa Megaunit. *Tectonophysics* 363, 201–224.

Molnár F. 1996: Fluid inclusion characteristics of Variscan and Alpine metallogeny of the Velence Mts., W-Hungary. In: Plate tectonic aspects of the Alpine metallogeny in the Carpatho-Balkan Region. *Proceedings of the Annual Meeting Sofia 1996* 2, 29–44.

Molnár F. 1997: Contribution to the genesis of molybdenite in the Velence Mts.: mineralogical and fluid inclusion studies on the mineralization of the Retezi audit. *Bull. Hung. Geol. Soc.* 127, 1–2, 1–17.

Molnár F. 2004: Characteristics of Variscan and Palaeogene fluid mobilization and ore forming processes in the Velence Mts., Hungary: A comparative fluid inclusion study. *Acta Mineral. Petrogr.* 45, 1, 55–63.

Molnár F., Török K. & Jones P. 1995: Crystallization conditions of pegmatites from the Velence Mts., Western Hungary, on the basis of thermobarometric studies. *Acta Geol. Hung.* 38, 1, 57–80.

Nemecz E. 1973: Clay minerals. *Academic Press,* Budapest, 1–507.

Oakes C.S., Bodnar R.J. & Simonson J.M. 1990: The system $NaCl–CaCl_2–H_2O$: I. The ice liquidus at 1atm total pressure. *Geochim. Cosmochim. Acta* 54, 603–610.

Pamić J.J. 1984: Triassic magmatism of the Dinarides in Yugoslavia. *Tectonophysics* 109, 273–307.

Parry W.T. & Jasumback M. 2002: Clay mineralogy of phyllic and intermediate argillic alteration at Bingham, Utah. *Econ. Geol.* 97, 221–239.

Reyes A.G. 1990: Petrology of Philippine geothermal systems and the application of alteration mineralogy to their assessment. *J. Volcanol. Geotherm. Res.* 43, 279–309.

Richards J.P. & Noble S.R. 1998: Application of radiogenic isotope systems to the timing and origin of hydrothermal processes. *Rev. Econ. Geol.* 9–10, 199–233.

Scroll E. & Pak E. 1983: Sulfur isotope investigations of ore mineralizations of the Eastern Alps. In: Schneider J.H. (Ed.): Mineral deposits of the Alps and of the Alpine Epoch in Europe. *Springer,* Berlin, Heidelberg, 169–175.

Schuster R., Scharbert S. & Abart R. 1999: Permo-Triassic crustal extension during opening of the Neotethyan-ocean in the Austroalpine–South Alpine realm. *Tüb. Geowiss. Arb.* 52, 5–6.

Stacey J.S. & Kramers J.D. 1975: Approximation of terrestrial lead isotope evolution by a two-stage model. *Earth. Planet. Sci. Lett.* 26, 207–221.

Szakáll S. & Molnár F. 2003: Primary and secondary minerals of the Szabadbattyán ore deposit (W-Hungary). In: Szakáll S. & Fehér B. (Eds.): Minerals of the Szár Hill Polgárdi, Hungary. *Herman Ottó Museum*, Miskolc, 145–175.

Środoń J. 1984: X-ray powder diffraction identification of illitic materials. *Clays and Clay Miner.* 32, 5, 337–349.

Tari G. 1996: Neoalpine tectonics of the Danube Basin (NW Pannonian Basin, Hungary). In: Ziegler P.A. & Horváth F. (Eds.): Peri-Thetys Memoir 2: Structure and prospects of Alpine basins and forelands. *Mem. Mus. Nat. Hist. Natur.* 170, 439–454.

Uher P. & Broska I. 1994: The Velence Mts. granitic rocks: geochemistry, mineralogy and comparison to Variscan Western Carpathian granitoids. *Acta Geol. Hung.* 37, 45–66.

Uher P. & Broska I. 1996: Post-orogenic Permian granitic rocks in the Western Carpathian-Pannonian area: Geochemistry, mineralogy and evolution. *Geol. Carpathica* 47, 311–321.

von Blanckenburg F. & Davies J.H. 1995: Slab breakoff: a model for syncollisional magmatism and tectonics in the Alps. *Tectonics* 14, 1, 120–131.

Vörös A. 1993: Jurassic microplate movements and brachiopod migrations in the western part of the Tethys. *Palaeogeogr. Palaeoclimatol. Palaeoecol.* 100, 125–145.

Zartman R.E. & Doe B.R. 1981: Plumbotectonics — The model. *Tectonophysics* 75, 135–162.

Zeeh S., Kuhlemann J. & Bechstädt T. 1998: The classical lead–zinc deposits of the eastern Alps (Austria/Slovenia) revisited: MVT deposits resulting from gravity driven fluid flow in the Alpine realm. *Geologija* 41, 257–273.

Zhang Y.G. & Frantz J.D. 1987: Determination of the homogenization temperatures and supercritical fluids in the system $NaCl–KCl–CaCl_2–H_2O$ using synthetic fluid inclusions. *Chem. Geol.* 64, 335–350.

Zhao M.W., Ahrendt H. & Wemmer K. 1997: K-Ar systematics of illite/smectite in argilliceous rocks from the Ordos basin, China. *Chem. Geol.* 136, 153–169.

Zwingmann H., Mancktelow N., Antognini M. & Lucchini R. 2010: Dating of shallow faults: New constraints from the AlpTransit tunnel site (Switzerland). *Geology* 38, 487–490.

Appendix A

Fluid inclusion data. **A** — Low salinity fluid inclusions modelled in the $NaCl+H_2O$ binary system.

Block	Locality	Host mineral	Host rock alteration	Fluid inclusion classifiacation	Th (°C)	Te (°C)	Tm (°C)	Salinity ($CaCl_2$ equiv. wt. %)
Eastern	Pákozd Line E	Granite, rock forming quartz	No alteration	Secondary	192	–48	–15.8	18.3
				Secondary	199	–47	–16.0	18.4
				Secondary	243			
				Secondary	246	–47	–16.0	18.4
				Secondary	214	–48	–16.0	18.4
				Secondary	226		–16.8	18.9
				Secondary	213		–15.6	18.2
				Secondary	239		–15.6	18.2
				Secondary	228		–8.8	13.2
				Secondary	229			
				Secondary	226			
				Secondary	218		–13.0	16.5
				Secondary	212	–48	–14.0	17.2
				Secondary	235			
				Secondary	185		–10.4	14.5
				Secondary	229		–15.0	17.8
				Secondary	204			
	Rigó Hill			Secondary	142	–50.2	–11.4	15.3
				Secondary	98	–48	–16.0	18.4
				Secondary	200		–17.0	19.0
				Secondary	151	–41	–12.8	16.4
				Secondary	120	–45	–20.3	20.8
				Secondary	151	–51	–19.8	20.6
				Secondary	170	–51	–11.1	15.1
				Secondary	144		–15.6	18.2
				Secondary	138	–50	–25.0	23.1
				Secondary	98	–45	–31.0	25.5
				Secondary	157	–57	–33.0	26.2
	Sorompó Valley			Secondary	160	–60	–28.0	24.3
				Secondary	205		–15.1	17.9
				Secondary	128	–56.6	–17.4	19.3
				Secondary	167	–56	–20.0	20.7
				Secondary	167	–56.6	–23.3	22.3
				Secondary	191	–53	–18.0	19.6
				Secondary	184	–55	–21.4	21.4
				Secondary	214	–57.2	–22.2	21.8
				Secondary	164	–51	–19.0	20.2
				Secondary	197	–57	–17.5	19.3
				Secondary	217	–53.7	–18.1	19.7
				Secondary	203		–18.3	19.8
				Secondary	211	–52	–17.6	19.4
	Zsellérek pasturale		Illite-kaolinite-smectite alteration and quartz veins	Secondary	137	–64.5	–28.4	24.5
				Secondary	200	–64	–28.1	24.4
				Secondary	155	–66	–20.6	21.0
				Secondary	158		–17.8	19.5
				Secondary		–66	–17.4	19.3
				Secondary	157	–57	–17.0	19.0
				Secondary		–58.8	–16.9	19.0
				Secondary	133	–27	–16.6	18.8
				Secondary	159	–60	–15.2	18.0
				Secondary	103	–65	–14.9	17.8
				Secondary	162	–65	–14.0	17.2
				Secondary	146	–57	–13.3	16.7
				Secondary	140			
				Secondary	157			
				Secondary	152			
				Secondary	172			
				Secondary	196			

Appendix B

Fluid inclusion data. **B** — High salinity fluid inclusions modeled in the $CaCl_2$+H_2O binary system.

Block	Locality	Host mineral	Host rock alteration	Fluid inclusion classifiacation	Th (°C)	Te (°C)	Tm (°C)	Salinity ($CaCl_2$ equiv. wt. %)
Western	Pátka South	Granite, rock forming quartz	No alteration	Secondary	113			
				Secondary	139	–51.2	–22.7	22.0
				Secondary	163		–21.7	21.5
				Secondary	166		–29.0	24.7
				Secondary	134		–28.7	24.6
				Secondary	112			
				Secondary	113			
				Secondary	116			
				Secondary	50			
				Secondary	108			
				Secondary	139			
				Secondary	134			
				Secondary	103		–20.9	21.1
				Secondary	113		–16.9	19.0
				Secondary	98		–23.0	22.2
				Secondary	118		–20.2	20.8
				Secondary	88		–14.9	17.8
				Secondary	114			
				Secondary	135		–9.4	13.7
				Secondary	118		–8.7	13.1
				Secondary	150		–21.9	21.6
				Secondary	119		–16.0	18.4
				Secondary	134			0.0
				Secondary	132		–16.0	18.4
				Secondary	74		–15.0	17.8
				Secondary	101		–14.0	17.2
	Székesfehérvár, lake		Illite-kaolinite-smectite alteration and quartz veins	Secondary	92	–33	–25.0	23.1
				Secondary	92			
				Secondary	115		–10.4	14.5
				Secondary	119		–23.7	22.5
				Secondary	87			
				Secondary	123	–50	–26.5	23.7
				Secondary	119	–48	–27.0	23.9
				Secondary	88	–48		
				Secondary	90		–15.0	17.8
				Secondary	97			
				Secondary	99	–47.6	–10.5	14.6
				Secondary	90			
				Secondary	75			
				Secondary	93			
				Secondary	81	–57	–30.5	25.3
				Secondary	82	–56.1	–25.0	23.1
				Secondary	133		–14.0	17.2
				Secondary	137			
				Secondary	118		–13.0	16.5
				Secondary			–24.5	22.9
				Secondary			–20.2	20.8
	Birkatanya			Secondary	289		–16.0	18.4
				Secondary	296		–5.8	10.0
				Secondary	282		–16.5	18.7
				Secondary	78		–13.9	17.12
				Secondary	113			
				Secondary	116	–47	–13.0	16.5
				Secondary	62		–14.7	17.64
	Pátka, Szűzvár mine	Sphalerite		Primary	105	–53.6	–17.0	19.03
				Primary	105	–53.1	–16.9	18.97
				Primary	112			
				Primary	109	–53	–16.7	18.86
				Primary	106	–50.7	–17.3	19.2
				Primary	109	–50.4	–15.8	18.32
				Primary	93	–50.2	–16.8	18.92
				Primary	98	–56.6	–20.9	21.14
				Primary	84	–48.6	–19.0	20.15
				Primary	81	–48.7	–22.1	21.73
				Primary	85	–49.5	–20.8	21.09
				Primary	99	–51.7	–18.8	20.04
				Primary	96	–57.5	–17.0	19.03
				Primary	74	–55.1	–23.0	22.16
				Primary	87	–54	–16.4	18.68
	Pákozd block	Hydrothermal quartz		Secondary	138	–70	–24.7	22.94
				Secondary	159	–67	–25.4	23.23
				Secondary	204	–67	–26.0	23.51
				Primary	83	–20	–19.0	20.15
				Primary	90		–25.0	23.08
				Primary	90		–19.8	20.57
				Secondary	121		–23.2	22.26
				Secondary	175	–69	–26.7	23.81
				Secondary	166	–72	–24.6	22.9
				Primary	183	–78.5	–24.6	22.9
				Primary	78	–50.6	–16.1	18.5
				Primary	84	–56	–14.9	17.76
				Primary	80	–61.8	–15.7	18.26
				Primary	98			
				Primary	139			
				Primary	126			
				Primary	72	–51		
				Primary	81		–14.0	17.18
				Primary	81		–17.0	19.03
				Primary	89		–13.7	16.98